*Human Molecular Genetics*, 2016, Vol. 25, No. 10 1990–2004

**doi: 10.1093/hmg/ddw074**
Advance Access Publication Date: 2 March 2016
Original Article

ORIGINAL ARTICLE

# $mGlu_5$ positive allosteric modulation normalizes synaptic plasticity defects and motor phenotypes in a mouse model of Rett syndrome

Rocco G. Gogliotti[1,2], Rebecca K. Senter[1,2], Jerri M. Rook[1,2], Ayan Ghoshal[1,2], Rocio Zamorano[1,2], Chrysa Malosh[1,2,4], Shaun R. Stauffer[1,2,4,5], Thomas M. Bridges[1,2], Jose M. Bartolome[6], J. Scott Daniels[1,2], Carrie K. Jones[1,2], Craig W. Lindsley[1,2,4], P. Jeffrey Conn[1,2,3] and Colleen M. Niswender[1,2,3,*]

[1]Department of Pharmacology and [2]Vanderbilt Center for Neuroscience Drug Discovery, Vanderbilt University Medical Center, Nashville, TN 37232, USA, [3]Vanderbilt Kennedy Center, [4]Department of Chemistry and [5]Vanderbilt Institute of Chemical Biology, Vanderbilt University, Nashville, TN 37232, USA and [6]Neuroscience Medicinal Chemistry, Janssen Research and Development, Jarama 75A., Toledo 45007, Spain

*To whom correspondence should be addressed. Email: colleen.niswender@vanderbilt.edu

## Abstract

Rett syndrome (RS) is a neurodevelopmental disorder that shares many symptomatic and pathological commonalities with idiopathic autism. Alterations in protein synthesis-dependent synaptic plasticity (PSDSP) are a hallmark of a number of syndromic forms of autism; in the present work, we explore the consequences of disruption and rescue of PSDSP in a mouse model of RS. We report that expression of a key regulator of synaptic protein synthesis, the metabotropic glutamate receptor 5 ($mGlu_5$) protein, is significantly reduced in both the brains of RS model mice and in the motor cortex of human RS autopsy samples. Furthermore, we demonstrate that reduced $mGlu_5$ expression correlates with attenuated DHPG-induced long-term depression in the hippocampus of RS model mice, and that administration of a novel $mGlu_5$ positive allosteric modulator (PAM), termed VU0462807, can rescue synaptic plasticity defects. Additionally, treatment of *Mecp2*-deficient mice with VU0462807 improves motor performance (open-field behavior and gait dynamics), corrects repetitive clasping behavior, as well as normalizes cued fear-conditioning defects. Importantly, due to the rationale drug discovery approach used in its development, our novel $mGlu_5$ PAM improves RS phenotypes and synaptic plasticity defects without evoking the overt adverse effects commonly associated with potentiation of $mGlu_5$ signaling (i.e. seizures), or affecting cardiorespiratory defects in RS model mice. These findings provide strong support for the continued development of $mGlu_5$ PAMs as potential therapeutic agents for use in RS, and, more broadly, for utility in idiopathic autism.

## Introduction

Rett syndrome (RS) is a neurodevelopmental disorder that results from *de novo* mutations in the *methyl CpG binding protein 2* (*MECP2*) gene (1). As is true with many other syndromic forms of autism, the phenotypic and molecular etiology of RS has significant overlap with idiopathic forms of Autism Spectrum Disorder (ASD); in this regard, therapeutic development for RS is anticipated to have broad utility. Phenotypically, RS patients present with core ASD diagnostic criteria, such as verbal and non-verbal communication deficits, disrupted gait dynamics, characteristic

**Received:** October 22, 2015. **Revised:** February 4, 2016. **Accepted:** February 29, 2016

hand stereotypies, developmental regression and intellectual disability (2). Commonalities are also observed in synaptopathies, as high-frequency stimulation-induced long-term potentiation (LTP) is attenuated in *Mecp2*-deficient mice (3–8), and the expression of proteins central to synaptic transmission, such as the N-methyl-D-aspartate receptor (NMDAR) and the metabotropic glutamate receptor 5 ($mGlu_5$), have been reported to be decreased in the brains of similar models (9–11).

A separate aspect of disease etiology that is shared between RS and ASD is that of disrupted translation in neurons (12,13). Protein synthesis-dependent synaptic plasticity (PSDSP) is the process by which changes in neuronal activity evoke corresponding alterations in the rate of local transcription/translation within dendrites (14). This results in remodeling of the synaptic architecture, AMPA receptor internalization, feedback signaling to the soma, as well as several other processes that affect synaptic transmission (15–19). These changes in synaptic plasticity can be measured as LTP or long-term depression (LTD), and persist for hours after the initial stimulation (17,20,21). Disruptions in PSDSP have been proposed to be disease-causing in syndromic forms of autism (i.e. Fragile X syndrome (FXS), Tuberous Sclerosis Complex (TSC), Neurofibromatosis Type 1 and Chromosome 16p11.2 microdeletion (18,22–24)), where normalization of this imbalance positively modifies disease and is currently the basis of multiple drug-development platforms.

With regard to RS, evidence suggests that decreased protein synthesis is an important aspect of disease progression (11–13). Protein synthesis-relevant pathways, such as the protein kinase B (ATK)/mammalian target of rapamycin (mTOR)/P70 S6 kinase (S6K) signaling axis, have been shown to be depressed in advanced stage *Mecp2* knockout mice (13,25) and in a human embryonic stem-cell neuronal model of RS (12). Furthermore, activation of AKT signaling in rodent models of RS with brain-derived neurotrophic factor (BDNF) mimetics (26,27) or recombinant human insulin-like growth factor 1 (IGF-1) (28) results in improvements in motor, cognitive and respiratory phenotypes, as well as normalized measures of synaptic plasticity. Both BDNF and IGF-1 have diverse signaling profiles and undoubtedly have effects that extend beyond AKT modulation; however, their shared effects on the same signaling pathway reinforce the potential utility of this therapeutic strategy.

In this study, we explore positive allosteric modulation of the $mGlu_5$ receptor as a means of normalizing PSDSP in *Mecp2*-deficient mice that is devoid of the broad signaling pathways associated with pleiotropic growth factors, which have been associated with adverse cardiovascular effects in some contexts (29). Metabotropic glutamate receptors are part of a superfamily of G protein-coupled receptors (GPCRs) represented by eight distinct subtypes ($mGlu_{1–8}$) (30), and $mGlu_5$ is a post-synaptic receptor with a well-characterized ability to modulate AKT-mediated protein synthesis pathways (17,18,31–33). Based on this ability, a number of $mGlu_5$ negative allosteric modulators with drug-like properties have been generated for diseases of excess PSDSP (i.e. FXS) (16,34–36), while $mGlu_5$ positive allosteric modulator (PAM) drug development has progressed at much slower pace. The primary cause of this delay in progression is highlighted by several reports (37,38) that discuss the presence of target-mediated excitotoxicity and severe, generalized seizures induced by certain $mGlu_5$ PAMs. Thus, despite a clear biological rationale for $mGlu_5$ potentiation in diseases like TSC and RS, very few $mGlu_5$ PAMs have advanced in development. However, it has also been demonstrated that these excitotoxic challenges can be mitigated by optimizing compounds that are free of direct agonist activity in the absence of an orthosteric ligand (38) and that do not potentiate $mGlu_5$ modulation of NMDA receptors or enhance hippocampal LTP (39). Building upon these discoveries, we describe VU0462807, an $mGlu_5$ PAM that has drug-like properties and a large enough therapeutic window to support chronic dosing paradigms in rodents. Furthermore, we demonstrate that $mGlu_5$ expression is reduced in *Mecp2* knockout mice and in the motor cortex of autopsy samples from RS patients, suggesting that reduced $mGlu_5$ signaling is a translationally relevant finding. Importantly, treatment with our novel $mGlu_5$ PAM in *Mecp2* knockout mice rescues attenuated PSDSP, improves motor performance and normalizes fear-conditioning deficits. This benefit is observed in a vulnerable disease model in the absence of any overt adverse effects, thereby providing strong support for the continued development of $mGlu_5$ PAMs as potential RS therapeutic agents, as well as for other disorders where PSDSP is reduced.

## Results

### Development of VU0462807 as a novel $mGlu_5$ PAM

Building upon recent advances in $mGlu_5$ drug discovery, we have developed a novel $mGlu_5$ PAM, termed VU0462807 (Fig. 1A). As was true with a previously reported $mGlu_5$ PAM, VU0361747 (green line) (38), VU0462807 (blue line) did not induce calcium mobilization in $mGlu_5$-R10A cells when applied alone, but potentiated the response of an $EC_{20}$ concentration of glutamate to 65% of the response elicited by a maximal concentration of glutamate ($Glu_{max}$) (Fig. 1B), suggesting that it is void of allosteric agonist activity in this assay. Conversely, the previously reported $mGlu_5$ agonist-PAM (ago-PAM), VU0424465, directly activated $mGlu_5$ when applied alone and induced a calcium mobilization response that measures 26% of the maximum response to glutamate (first peak observed in the pink trace, Fig. 1B) (38). *In vitro*, VU0462807 exhibits an $EC_{50}$ of 60 nM as a PAM and maximally shifts the glutamate concentration–response $4.2 \pm 0.27$ fold to the left (Fig. 1B and Supplementary Material, Fig. S1). The compound was inactive against all other mGlu receptor subtypes (<1.3-fold shift of an agonist concentration–response in either direction at 10 μM) (Supplementary Material, Fig. S2), and had a clean profile when assessed in a Ricerca binding panel of 67 distinct receptors, ion channels and transporters (40). Following a single 10 mg/kg intraperitoneal (IP) injection to C57Bl/6 mice, VU0462807 exhibited a maximum concentration ($C_{max}$) in the brain of 1836 ng/g and a $C_{max}$ in plasma of 1469 ng/ml, with a time to reach $C_{max}$ ($T_{max}$) of 0.25 h and an area under the curve (AUC) exposure of 400 ng/g*h and 320 ng/ml*h (*projected), respectively (Fig. 1C and Supplementary Material, Fig. S3). Moderately higher $C_{max}$ and exposures were observed in Sprague–Dawley rats following a single IP administration of the same dose (Supplementary Material, Fig. S3). In both species, the compound freely and rapidly distributed to the brain with total and estimated unbound brain:plasma partition coefficients ($K_p$, $K_{p,uu}$, respectively) of 1.12 and 1.56 (determined at 1.5 h) in rat and 1.25 and 1.75 (determined at 1 h) in mouse. *In vitro* plasma protein and brain homogenate assays revealed VU0462807 to possess high fraction unbound ($f_u$) values in rat plasma (0.372) and brain (0.517). Neither acute ($1 \times 1$ day) nor sub-chronic ($1 \times 4$ days) IP administration of 56.6 mg/kg VU0462807 had measureable adverse effects as assessed using Irwin Neurological battery in Sprague–Dawley rats (Supplementary Material, Table S1). Consistent with other $mGlu_5$ PAMs, VU0462807 decreased amphetamine-induced hyperlocomotion in rats in a dose-dependent manner from 0.3 to 30 mg/kg (Fig. 1D, and full concentration–response profile shown in Supplementary Material, Fig. S4) (15).

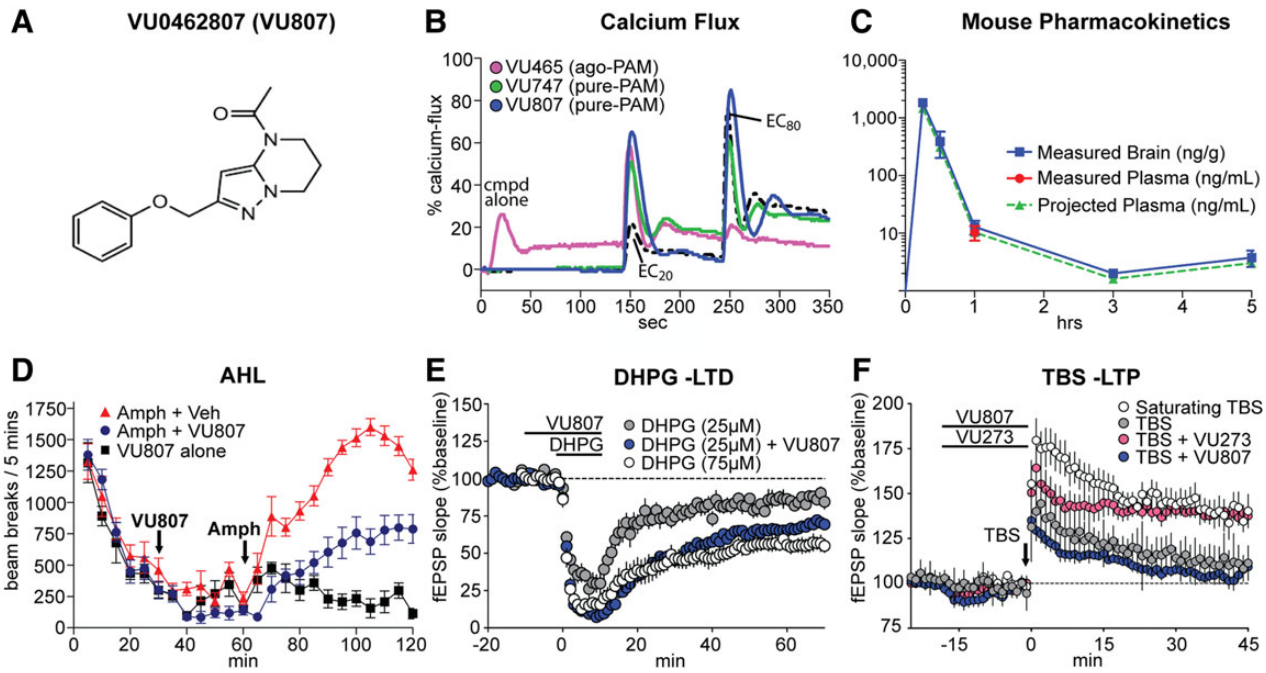


**Figure 1.** Characterization of VU0462807 (VU807), a novel $mGlu_5$ positive allosteric modulator. (**A**) Structure of VU0462807 (VU807). (**B**) 'Triple add' Calcium Flux assay. Representative calcium traces following the addition of 30 μM VU0424465 (VU465, pink), VU0361747 (VU747, green) or VU0462807 (VU807, blue), followed by a concentration of glutamate eliciting a 20% maximal response ($EC_{20}$), and an 80% maximal response ($EC_{80}$). Glutamate alone traces are in dashed black. Note that the agonist/positive allosteric modulator (PAM) VU465 evokes calcium flux when added alone, but the PAMs VU747 and VU807 only potentiate an $EC_{20}$ concentration of glutamate. (**C**) Following a single 10 mg/kg IP administration to male C57Bl/6 mice ($N = 3$), VU807 reached a maximal concentration ($C_{max}$) in the brain of 1836 ng/g and the plasma of 1469 ng/ml (*projected) at a $T_{max}$ of 0.25 h with an $AUC_{0-last}$ of 400 ng/g*h and 320 ng/ml*h (*projected), respectively. Mouse plasma concentrations projected based on a mouse brain:plasma $K_p$ of 1.25 at the 1 h time-point in this study. (**D**) 30 mg/kg VU807 (IP) attenuates amphetamine (amph) induced hyperlocomotion (AHL) in WT rats. VU807 + amph (blue circles), vehicle + amph (red triangles), vehicle alone (black square). Over the final 60 min of the test, vehicle + amph-treated mice averaged 1340 beam breaks/5 min, and this was significantly reduced to 672.3 beam breaks/5 min in the 30.0 mg/kg VU807 + amph-treated cohort (***$P \leq 0.001$, Student's *t*-test). $N = 7$/group. Full VU807 dose–response in the amphetamine model is shown in Supplementary Material, Figure S4. (**E**) DHPG-induced long-term depression (LTD) at the SC-CA1 synapse. The response to a threshold concentration (25 μM) of DHPG (gray, 82.7 ± 2.5% of baseline at 60 min) can be potentiated into a LTD comparable to saturating conditions [white, 55.0 ± 4.5% (75 μM)] with 30 μM VU807 pre-treatment (blue, 67.8 ± 2.6%). (**F**) One train of theta burst stimulation (TBS) induced a long-term potentiation (LTP) response at the SC-CA1 synapse. Stereotypical $mGlu_5$ PAMs, like VU0092273, potentiate TBS-induced LTP to a near saturating response (pink circles); white circles show response to a saturating stimulation protocol. However, VU807 (blue circles) has no effect on this NMDAR-mediated form of LTP, which is indicative of signal bias.

To assess a protein synthesis-dependent form of synaptic plasticity, we examined (S)-3,5-Dihydroxyphenylglycine (DHPG)-induced LTD at the SC-CA1 synapse in the hippocampus (17,18), and found that 30 μM VU0462807 potentiated the response to a sub-threshold concentration of DHPG (25 μM), eliciting robust LTD (67.8 ± 3% of baseline) 60 min after addition of DHPG and VU0462807 (Fig. 1E). We next assessed the effects of VU0462807 on theta-burst stimulation (TBS)-induced LTP at SC-CA1 synapses. In the presence of vehicle, the field excitatory post-synaptic potential (fEPSP) slope measured 45 min after threshold TBS was 111 ± 3% of baseline. Conversely, slices perfused with a prototypical, non-biased $mGlu_5$ PAM, VU0092273 (41), presented with an LTP response that was 140 ± 4% of the baseline at 45 min post-stimulation (Fig. 1F). In contrast, VU0462807 failed to potentiate the LTP response measured 45 min after threshold TBS (104 ± 3% of the baseline, Fig. 1F). This lack of effect of VU0462807 is similar to our previously reported biased compound, VU0409551 (39), and suggests that the compound does not potentiate NMDA receptor-dependent forms of synaptic transmission at the SC-CA1 synapse.

## $mGlu_5$ expression is reduced in advanced stage *Mecp2*$^{-/y}$ mice and RS patients

Previous studies have demonstrated reduced $mGlu_5$ expression in *ex vivo* hippocampal slices from *Mecp2*$^{S421A/S424A/y}$ knock-in mice (11). To confirm these findings in a more broadly used model and to help establish rationale for testing $mGlu_5$ PAMs in RS, we harvested total cortex, hippocampus and striatum, and microdissected motor cortex from P10, P30 and P50 *Mecp2*$^{+/y}$ and *Mecp2*$^{tm1.1Bird/y}$ male mice (referred to hereafter as *Mecp2*$^{-/y}$) and assessed *Grm5* expression via quantitative real-time PCR (QRT-PCR). Using this approach, we observed that *Grm5* expression was only reduced at advanced stages (P50) in the motor cortex (77.0 ± 4.2%, $P \leq 0.05$), the hippocampus (60.5 ± 11.8%, $P \leq 0.05$) and in the striatum (45.2 ± 5.7%, $P \leq 0.01$) (Fig. 2A–D). Changes in *Grm5* expression were not observed in the total cortex, suggesting that the reductions quantified in motor cortex were diluted out by the larger sample volume (Fig. 2A). These findings were subsequently confirmed by western blot, as reduced $mGlu_5$ levels were quantified in the motor cortex (64.6 ± 4.7%, $P \leq 0.01$), hippocampus (86.4 ± 2.8%, $P \leq 0.01$) and striatum (64.4 ± 2.1%, $P \leq 0.001$) (Fig. 2E and F). Interestingly, and in contrast to advanced stage *Mecp2*$^{-/y}$ mice, we observed significant increases in *Grm5* expression at P10 in the hippocampus (134.0 ± 10.1%, $P \leq 0.05$) and at P30 in the striatum (235.7 ± 71.4%, $P \leq 0.05$); potentially indicative of biphasic regulation of *Grm5* gene expression (Fig. 2C and D).

To determine whether the changes observed in rodents could be translated to human-derived cells, we next examined $mGlu_5$ expression using MeCP2 deficient human induced pluripotent stem cell (iPSC)-derived neurons. In this commercially available,

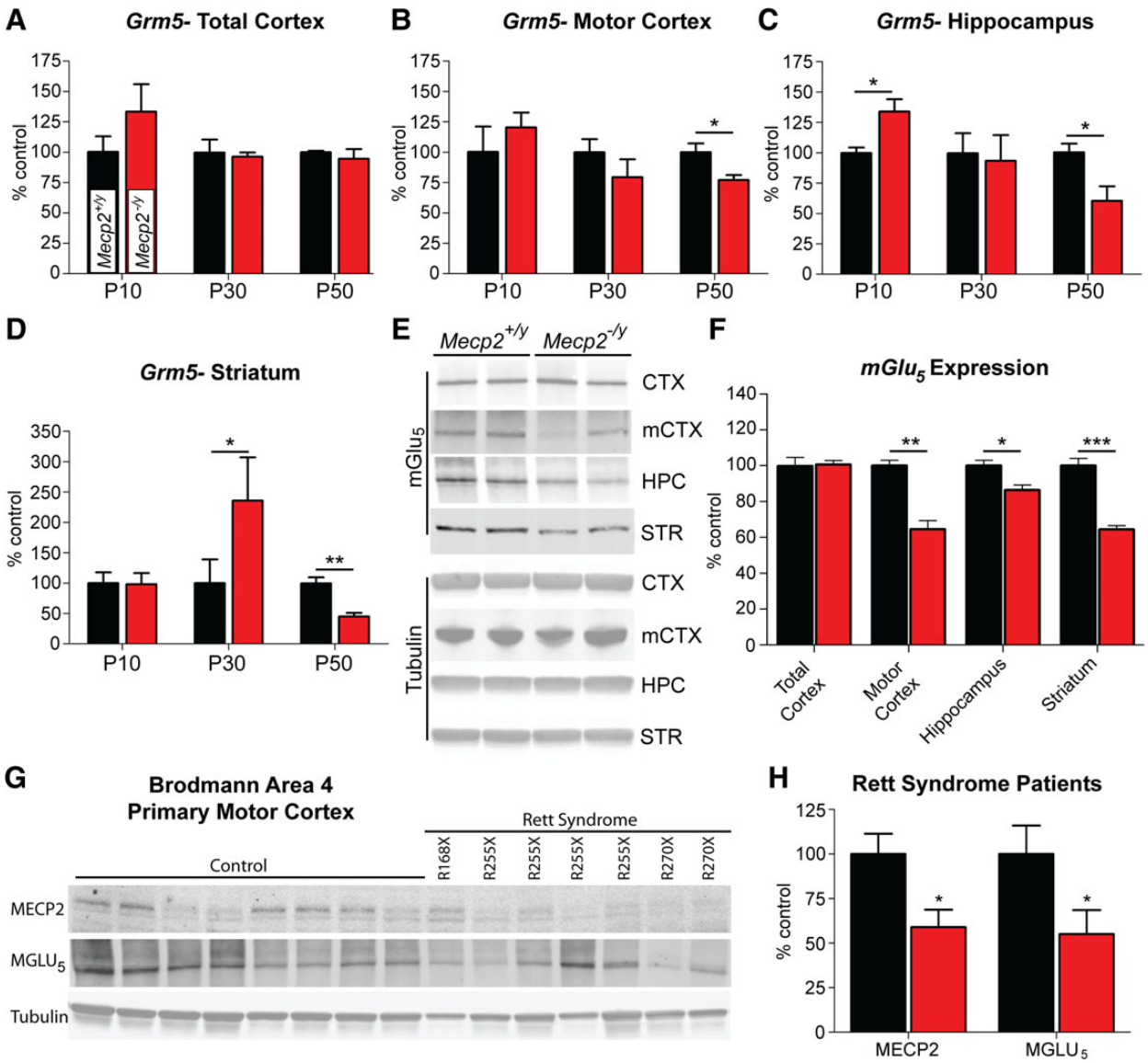


**Figure 2.** BTemporal and spatial Grm5/mGlu5 expression in Mecp2-/y mice and Rett syndrome autopsy samples. (**A**–**D**) Relative to $Mecp2^{+/y}$ mice, *Grm5* expression is significantly reduced in $Mecp2^{-/y}$ mice at P50 in the motor cortex (77.0 ± 4.2%, $^{*}P \leq 0.05$), hippocampus (60.5 ± 11.9%, $^{*}P \leq 0.05$) and striatum (45.2 ± 5.7%, $^{***}P \leq 0.001$), but not in total cortex (94.6 ± 8.0%, *ns*). *Grm5* expression is not decreased at time-points preceding P50, and is significantly increased at P10 in the hippocampus (134.0 ± 10.1%, $^{*}P \leq 0.05$) and at P30 in the striatum (235.7 ± 71.4%, $^{*}P \leq 0.05$), potentially indicating a biphasic shift in how *Grm5* expression is altered in response to Mecp2 deficiency. Two-way ANOVA with Bonferroni post-test. (**B** and **C**) $mGlu_5$ protein was reduced in the motor cortex (64.6 ± 4.7%, $^{**}P \leq 0.01$), hippocampus (86.4 ± 2.8% of $Mecp2^{+/y}$, $P \leq 0.05$) and striatum (64.4 ± 2.1% of $Mecp2^{+/y}$, $P \leq 0.001$), while there was no statistical difference in total cortex (101 ± 2.3% of $Mecp2^{+/y}$). Two-way ANOVA with Bonferroni post-test. (**D** and **E**) MeCP2 protein was reduced in the Brodmann area 4 (BA4, primary motor cortex) region of Rett syndrome autopsy samples (100 ± 11.4% control versus 59.0 ± 9.8% Rett syndrome, $^{*}P \leq 0.05$, Student's *t*-test), as were MGLU5 protein levels (100 ± 16.0% control versus 55.1 ± 13.4% Rett syndrome, $^{*}P \leq 0.05$, Student's *t*-test). Patient mutations are noted above each lane. $N = 8$ control, $N = 7$ Rett syndrome.

*in vitro* model of RS, *MECP2* has been deleted in a stable fibroblast line and then de-differentiated into a pluripotent lineage [Cellular Dynamics International (CDI)]. iPSCs were differentiated to a neuron-like lineage through culture in media containing a proprietary cocktail from CDI, a protocol known to produce cells with neuronal morphology and synaptic connections (42). After 14 days of culture in neuronal differentiation media, control and MeCP2-deficient neuron-like cells were harvested, and western blot analysis confirmed a 28 ± 1.5% ($P \leq 0.05$) reduction in $mGlu_5$ protein expression relative to control cells (Supplementary Material, Fig. S5).

To further confirm the translatability of decreased $mGlu_5$ expression, we obtained Brodmann area 4 (BA4) samples from seven RS patients and eight controls as a generous gift from Rettsyndrome.org, the Harvard Brain Tissue Resource Center and the University of Maryland Brain and Tissue Bank. The BA4 region mirrors our mouse data in that it encompasses primary motor cortex and is a cortical sub-region where strong pathology has been observed in RS patients (43–45). RS samples were derived from patients with a mean age of 16.0 ± 2.3 years and a post-mortem interval (PMI) of 10.5 ± 2.5 h. Control samples were from individuals with a mean age of 18.8 ± 3.9 years and a PMI of 17.0 ± 2.8 h. To obtain a homogeneous sample, BA4 tissue was mechanically dissociated under dry ice, pulverized under liquid nitrogen and then processed using standard western blotting procedures. Consistent with their known *MECP2* mutations,

MECP2 protein was significantly reduced in RS patient samples (59.0 ± 9.8% RS versus 100 ± 11.4% control, $P \leq 0.05$). Adding further support to the translatability of our findings in mice, $MGLU_5$ protein was also found to be significantly decreased in the BA4 region of RS patients (55.1 ± 13.4% RS versus 100 ± 16.0% control, $P \leq 0.05$). It is of note that no direct correlation could be established within the current data set between the amount of MECP2 and mutation location and/or $mGlu_5$ expression level, which may indicate that mutations in MECP2 alter $MGLU_5$ expression at a network level as opposed to direct binding to the *GRM5* locus.

## Compound selection and seizure liability

Reduced $mGlu_5$ expression, combined with the symptomatology and synaptopathology of RS, provide strong rationale for the examination of $mGlu_5$ PAMs as potential therapeutic agents in the treatment of RS. However, it is important to note that both RS patients and model mice are susceptible to spontaneous and induced epileptiform activity, which may indicate an increased vulnerability to adverse effects from ligands that potentiate glutamatergic signaling (46,47). Thus, it is possible that an $mGlu_5$ PAM with a favorable safety profile in a *C57/B6* mouse may still evoke adverse effects in a susceptible disease model. To address these concerns, we first conducted a primary screen of both novel and commonly used $mGlu_5$ PAMs in the inbred *FVBN* strain of mice, which exhibits a well-established seizure susceptibility (48,49). Specifically, we dosed 6-week-old *FVBN* male mice with the $mGlu_5$ PAMs VU0361747 (10 mg/kg) (38), VU0462807 (10 mg/kg), CDPPB (10 mg/kg) (50), the $mGlu_5$ allosteric ago-PAM VU0424465 (1 mg/kg) (38) and vehicle (10% Tween 80). Mice were then scored based on a Racine Scale (38) once every 5 min over the span of 1 h, with the scorer blinded to the treatment group. In agreement with our previous study in *C57/B6* mice, the $mGlu_5$ ago-PAM VU0424465 induced strong behavioral convulsions in *FVBN* mice (Fig. 3A; pink line) (38). Likewise, we also observed forelimb and facial clonuses with the commonly used $mGlu_5$ PAM, CDPPB (orange line), which corresponded to its known pharmacokinetic properties and *in vitro* agonist activity (51) (Fig. 3A). In the same manuscript as our VU0424465 study, we also reported that the $mGlu_5$ PAM VU0361747 did not evoke convulsive side effects in *C57/B6* mice (38). This was postulated to be related to the lack of agonist activity induced by the compound in *in vitro* calcium mobilization assays (Fig. 1B). However, when VU0361747 was administered to *FVBN* mice, we observed 1–2 forelimb and/or facial clonuses at points that corresponded with maximal *in vivo* brain concentrations (15 min, green line, Fig. 3A), indicating a seizure liability of this compound in hypersensitive models. In stark contrast, we observed no overt convulsive events when the novel $mGlu_5$ PAM VU0462807 was administered to *FVBN* mice (blue line, Fig. 3A).

Based on its favorable *in vivo* profile and lack of convulsive effects in *FVBN* mice, we advanced VU0462807 into studies in *Mecp2*$^{-/y}$ mice. We chose to test VU0462807 in advanced-stage *Mecp2*$^{-/y}$ mice because this genotype represents the most severe model of the disease and likely represents the most vulnerable test group (5). Advanced stage RS was phenotypically defined as

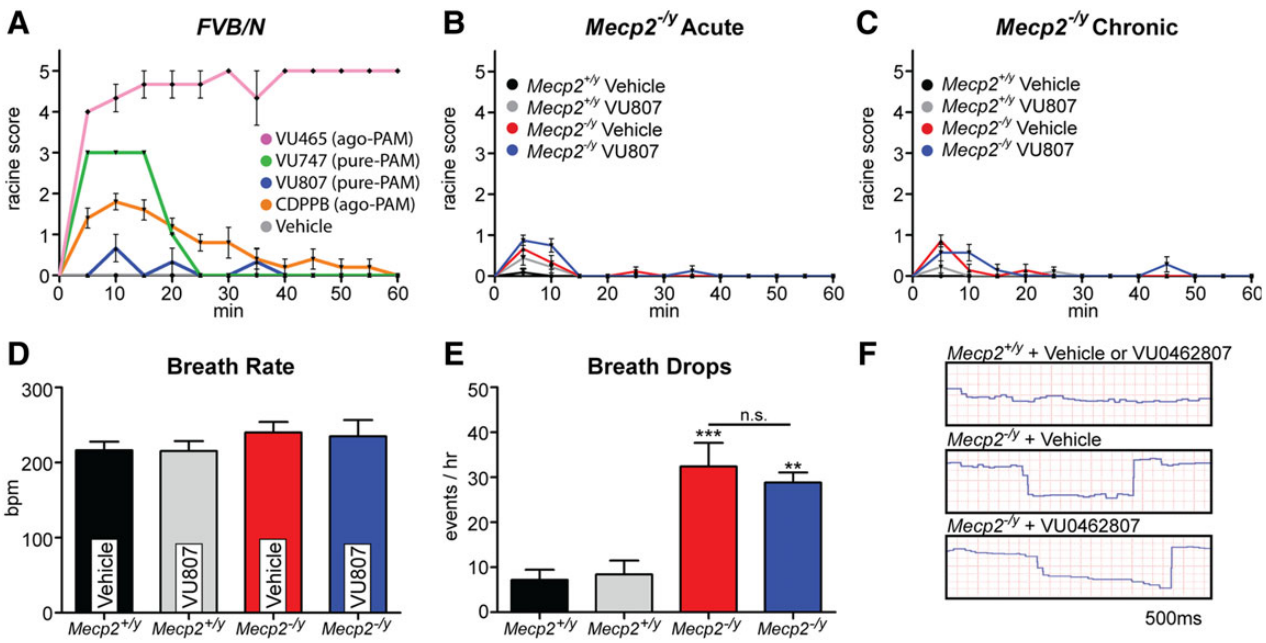


**Figure 3.** VU0462807 (VU807) does not evoke overt behavioral convulsions or alter respiratory function in *Mecp2*$^{-/y}$ mice. (**A–C**) Blinded Racine Score. (A) Primary screen for $mGlu_5$-mediated seizures in the hypersensitive *FVB/N* strain of mice (6-week-old, male). We observed a strong induction of generalized seizures with the ago-PAM VU0422465 (VU465, pink, 10 mg/kg) and a modest induction of limb and facial clonuses with CDPPB (orange, 10 mg/kg), which is also known to have agonist and PAM, activity *in vitro* (ago-PAM). Unexpectedly, an $mGlu_5$ PAM with no apparent *in vitro* allosteric agonist activity (pure-PAM), VU0361747 (VU747, green, 10 mg/kg), evoked 1–2 forelimb clonuses at $T_{max}$ (15 min), suggesting that epileptiform activity has not been fully eliminated from this compound in sensitive populations. Importantly, we observed no generalized seizures or convulsive behavior when VU807 (blue, 10 mg/kg) was dosed to *FVB/N* mice. ($N = 5$/compound, all compounds dosed IP) (B and C) VU807 (3.3 mg/kg, IP) was then progressed to studies in advanced stage P39 *Mecp2*$^{-/y}$ mice, where no induction of convulsive behavior was seen with either acute (B) or chronic (17 days, P39–55) (C) dosing. (**D–F**) Pulse Oximetry. (D) No significant difference in breath rate was observed between P55 *Mecp2*$^{+/y}$ and *Mecp2*$^{-/y}$ mice regardless of treatment. (E and F) Breathing irregularities. During assessment of breath rate, prolonged periods where the breath rate dropped to near zero were observed. These were quantified as occurring 32.4 ± 5.2 times per hour in vehicle-treated *Mecp2*$^{-/y}$ mice (***$P \leq 0.001$, relative to veh—*Mecp2*$^{+/y}$) and 28.8 ± 2.2 times per hour in VU807-treated *Mecp2*$^{-/y}$ mice (3.3 mg/kg) (**$P \leq 0.01$), which was not significantly different from vehicle-treated *Mecp2*$^{-/y}$ mice. $N = 5$/group. One-way ANOVA with Bonferroni post-test.

the point at which hind-paw clasping or knuckling persisted for >15 s per min when the mouse was suspended by its tail, with P39 representing the median age at which these criteria were reached in our colony. To determine if VU0462807 exhibited convulsive properties in this strain, P39 *Mecp2*$^{-/y}$ mice were dosed once-daily (QD) with 3.3 mg/kg VU0462807 or vehicle (10% Tween 80 in water) for 17 consecutive days. On Days 1 and 17, mice were scored in a blinded fashion, using a Racine scale, every 5 min for a period of 1 h after compound administration to represent acute and chronic VU0462807 treatment, respectively. As was true in the hypersensitive *FVB/N* strain, VU0462807 acute treatment did not evoke any overt behavioral convulsions in *Mecp2*$^{-/y}$ mice (Fig. 3B). This finding was mirrored in the chronic 17-day treatment group, which also demonstrated no overt convulsive behavior (Fig. 3C), suggesting that the compound possesses a favorable safety profile with regard to overt seizures.

## Cardiorespiratory phenotypes are unaffected by VU0462807

Beyond increased seizure susceptibility, *Mecp2*$^{-/y}$ mice also parallel RS patients in that they present with increased risk for cardiorespiratory dysfunction. Since disruption of the excitatory–inhibitory (E–I) balance within brain stem nuclei is believed to be one cause of respiratory dysfunction in mouse models of RS (52), and peripheral $mGlu_5$ expression has been reported in the heart (53), we posited that $mGlu_5$ PAMs might exacerbate cardiorespiratory phenotypes in this sensitive population. To address this concern, we performed pulse oximetry on advanced stage P55 *Mecp2*$^{-/y}$ and *Mecp2*$^{+/y}$ mice that were treated via IP injection once daily with 3.3 mg/kg VU0462807 or vehicle from P39 to P54. Mice were allowed to acclimate to the chamber and recording collar for 2 h, injected with compound one final time (P55) and then monitored for 10 min at the $T_{max}$ of the compound (15 min). In agreement with the findings of other labs, breath rate was not significantly different between vehicle-treated control (216 ± 11.5 breaths per min (bpm)) and *Mecp2*$^{-/y}$ mice (240 ± 14.0 bpm). This finding also held true in VU0462807-treated control (215 ± 13.2 bpm) and *Mecp2*$^{-/y}$ mice (235 ± 21.9 bpm) (Fig. 3D). Interestingly, we observed numerous points during recording where the respiratory rate of *Mecp2*$^{-/y}$ mice dropped to near zero for a period of 0.5–1.5 s (Fig. 3E and F). These irregularities were quantified by a blinded reviewer and calculated to appear in *Mecp2*$^{-/y}$ mice an average of 32.4 ± 5.2 times per hour in the vehicle-treated group, and 28.8 ± 2.2 times per hour in VU0462807-treated group (Fig. 3E and F), which was not statistically different. As a final safety assessment, we examined the effects of VU0462807 on the heart rate of *Mecp2*$^{-/y}$ mice. We observed significant bradycardia in *Mecp2*$^{-/y}$ mice relative to control mice, and this parameter was also unaffected by our novel $mGlu_5$ PAM (Supplementary Material, Fig. S6). Based on the results of these pulse oximetry experiments, we conclude that baseline cardiorespiratory dysfunction is unaffected by VU0462807 in advanced stage *Mecp2*$^{-/y}$ mice, and that the subsequent assessments of efficacy are not likely to be affected by overt adverse effects from VU0462807 treatment.

## VU0462807 corrects deficits in fear conditioning in *Mecp2*$^{-/y}$ mice

Mechanistically, it has been proposed that $mGlu_5$ potentiation may be beneficial in the enhancement of cognition, a known deficit in RS. As we observed reduced $mGlu_5$ expression in the hippocampus of *Mecp2*$^{-/y}$ mice, we hypothesized that potentiation of $mGlu_5$ might be efficacious in domains of learning and memory. To assess the effects of VU0462807 on cognition, we utilized both cued and contextual conditioned fear. 10 *Mecp2*$^{+/y}$ and 10 *Mecp2*$^{-/y}$ mice were injected (IP) with either VU0462807 or vehicle and placed in a conditioning chamber containing 1.0 ml of 10% vanilla in water. They were then subjected to two cycles of a 30 s tone followed by a brief foot shock (0.70 mA). Twenty-four hours later, mice were placed in the same chamber for a period of 4 min to assess contextual fear, and then, 1 h later, were placed in a novel chamber containing 1.0 ml of 10% almond scent in water and a 1 min tone was played to assess cued fear. In both situations, the amount of time spent freezing in response to the context or cue served as the outcome measure. Consistent with previous studies, vehicle-treated *Mecp2*$^{-/y}$ mice exhibited a modest reduction in contextual fear conditioning that failed to reach significance; in contrast, vehicle-treated *Mecp2*$^{-/y}$ animals showed a dramatic reduction in cued fear conditioning (Fig. 4A). Relative to vehicle-treated *Mecp2*$^{-/y}$ mice, VU0462807 significantly increased the percent of time spent freezing in response to both the contextual and cued stimulus (Fig. 4A), suggestive of improved cognition.

## VU0462807 improves motor function in *Mecp2*$^{-/y}$ mice

Based on our observation of reduced $mGlu_5$ expression in the striatum of *Mecp2*$^{-/y}$ mice and in the motor cortex of RS patients, we next assessed the benefit of VU0462807 on motor function. *Mecp2*$^{+/y}$ and *Mecp2*$^{-/y}$ mice were treated with either VU0462807 or vehicle, IP, QD from P47 to P54, and then monitored in an open-field for 60 min following compound administration. A chronic, rather than acute, dosing paradigm was chosen to allow time for motor learning to occur (54–57). As has been previously reported (5), vehicle-treated *Mecp2*$^{-/y}$ mice explored significantly less than *Mecp2*$^{+/y}$ mice, regardless of treatment (Fig. 4B); however, VU0462807 treatment normalized exploratory behavior in *Mecp2*$^{-/y}$ mice to that of wild-type controls (Fig. 4B). Additionally, the number of entries into the vertical place was significantly decreased in vehicle-treated *Mecp2*$^{-/y}$ mice, and this parameter of open-field was also rescued by chronic treatment with VU0462807 (Fig. 4C). Finally, we analyzed the percent time spent in the center of the open-field chamber and found no difference between vehicle-treated control and mutant mice; however, chronic treatment with VU0462807 significantly increased the percentage of time spent in the center in only *Mecp2*$^{-/y}$ mice, suggestive of anxiolytic properties that are specific to treatment in RS model mice, as compound treatment had no effect in wild-type mice (Fig. 4D).

Next, we performed high-speed ventral plane videography to further explore the effect of $mGlu_5$ potentiation on motor function in *Mecp2*-deficient mice. A baseline gait assessment was made prior to treatment (P35) to establish that no phenotypic difference existed between groups of *Mecp2*$^{-/y}$ mice, and the effects of chronic VU0462807 treatment (P39–P54, IP, QD) were then quantified at P54. Of the four core parameters of gait (stance, propel, swing and break), only the propel phase was significantly decreased in vehicle-treated *Mecp2*$^{-/y}$ mice (Fig. 4E–I). Beneficially, propel time was significantly increased to wild-type levels following chronic VU0462807 treatment; however, this value fell to vehicle-treated levels during post-treatment time-points, suggesting that the benefits of compound treatment are not sustained beyond the dosing window (Fig. 4E). Given that gait initiation has been demonstrated to be altered in RS patients, the normalization of gait dynamics may represent a preclinical outcome measure with translational value (58).

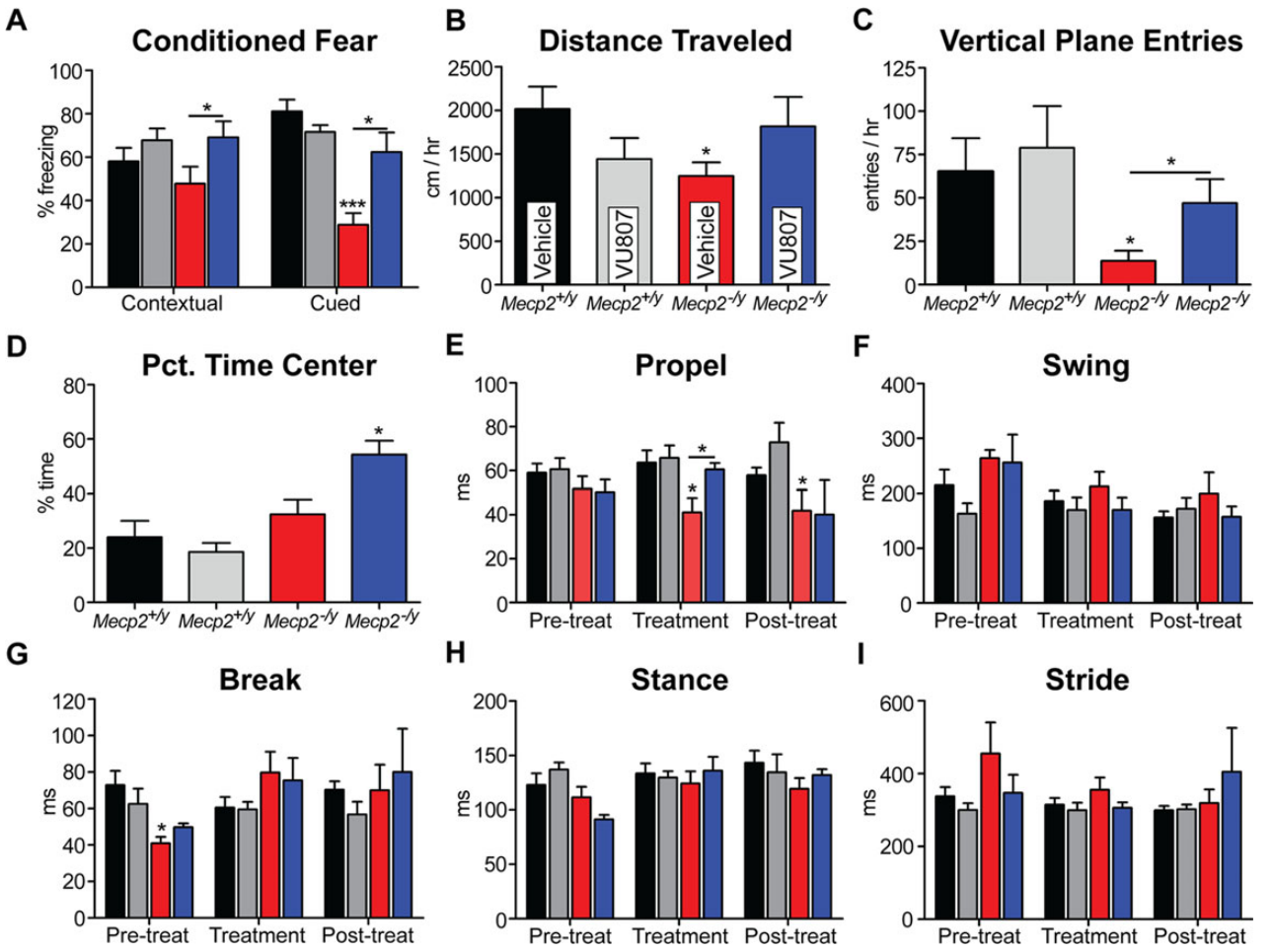


**Figure 4.** VU0462807 (VU807) improves conditioned fear, open-field and gait dynamics assays in *Mecp2*$^{-/y}$ mice. (**A**) Conditioned fear. Vehicle-treated *Mecp2*$^{-/y}$ mice froze 47.8 ± 7.9% of the time in the contextual fear assay relative to 58.0 ± 6.2% in vehicle-treated *Mecp2*$^{+/-}$ mice, which was significantly increased to 69.1 ± 7.4% with acute VU807 treatment (IP, $^{*}P \leq 0.05$). Conversely, cued fear conditioning was dramatically reduced in vehicle-treated Mecp2$^{-/y}$ mice (28.8 ± 5.3% of time spent freezing) relative to controls (71.6 ± 3.2%, $^{***}P \leq 0.001$, WT versus *Mecp2*$^{-/y}$), and this parameter was also significantly increased to 62.4 ± 9.0% with acute VU807 treatment ($^{*}P \leq 0.05$, *Mecp2*$^{-/y}$ vehicle versus VU807-treated). Two-way ANOVA with Bonferroni post-test. (**B–D**) Open-field assay. (B) Vehicle-treated *Mecp2*$^{-/y}$ mice explored an average of 1250 ± 156 cm/h, which was significantly less than the 1810 ± 298 cm/h observed in *Mecp2*$^{+/y}$ animals ($^{*}P \leq 0.05$, one-way ANOVA with Bonferroni post-test). Beneficially, chronic VU807 dosing normalized this parameter to 1815 cm/h in mutant mice, which was not statistically different than controls ($^{*}P \geq 0.05$). (C) Vertical plane entries per hour were significantly reduced in vehicle-treated *Mecp2*$^{-/y}$ mice (65.1 ± 19.0 *Mecp2*$^{+/y}$ versus 13.2 ± 5.8 *Mecp2*$^{-/y}$, $^{*}P \leq 0.05$, Two-way ANOVA with Bonferroni post-test), and this parameter was significantly improved to 47.0 ± 13.7 entries/h after VU807 treatment ($^{*}P \leq 0.05$ for vehicle versus VU807 treatment in *Mecp2*$^{-/y}$ mice). (D) *Mecp2*$^{+/y}$ and *Mecp2*$^{-/y}$ mice did not differ significantly in the percent time spent in the center region of the open-field assay; however, VU807-treated *Mecp2*$^{-/y}$ mice spent 54.3 ± 5.05% of the hour long test in the center of the testing apparatus, which was significantly longer than controls ($^{*}P \leq 0.05$). (**E–I**) High speed ventral plane videography. Of the four core parameters of gait, only the propel phase was significantly reduced in vehicle-treated *Mecp2*$^{-/y}$ mice (41.1 ± 6.5 ms, $^{*}P \leq 0.05$) relative to vehicle-treated *Mecp2*$^{+/y}$ mice (65.5 ± 5.1 ms, two-way ANOVA with Bonferroni post-test). Relative to vehicle-treated *Mecp2*$^{-/y}$ mice, VU807 corrected this abnormal aspect of gait dynamics to 60.6 ± 2.9 ms ($^{*}P \leq 0.05$) during treatment. Note that after the treatment had stopped, propel measurements returned to vehicle-treated levels (40.2 ± 15.5 ms).

## VU0462807 corrects clasping defects in male and female RS mice

During the course of chronic dosing for our motor function assays, it was noted that mice treated with VU0462807 spent significantly less time clasping their hind paws than animals treated with vehicle (Fig. 5A). To quantify this phenotype, *Mecp2*$^{-/y}$ and *Mecp2*$^{+/y}$ mice were again treated with vehicle and 3.3 mg/kg VU0462807 IP, QD from P39–P54. Mice were suspended by their tail and their hind-limb dynamics were recorded (i) prior to treatment on P36 to establish a baseline, (ii) three times during chronic treatment to assess compound efficacy and (iii) 5 days following treatment to identify any potential long-term treatment benefits (P57). The number of seconds per minute spent either clasping one or more paws, or knuckling the digits of the paw, was then scored by a researcher blinded to the treatment group. Prior to compound treatment, both groups of mutant mice demonstrated increased clasping (Fig. 5B). Remarkably, 3.3 mg/kg VU0462807 treatment once daily from P39 to P54 significantly decreased clasping at three separate time-points examined (P41, P47, P52), with vehicle-treated *Mecp2*$^{-/y}$ mice clasping a combined average of 37.5 ± 7.4 s/min and VU0462807-treated *Mecp2*$^{-/y}$ animals clasping an average of 9.0 ± 4.0 s/min (Fig. 5A and B; $P \leq 0.01$). Interestingly, this benefit was lost once treatment was stopped, and clasping returned levels that were not significantly different from vehicle treatment (38.0 ± 9.1 s/min in vehicle-treated mice versus 26.7 ± 7.7 s/min in VU0462807-treated mice) (Fig. 5B).

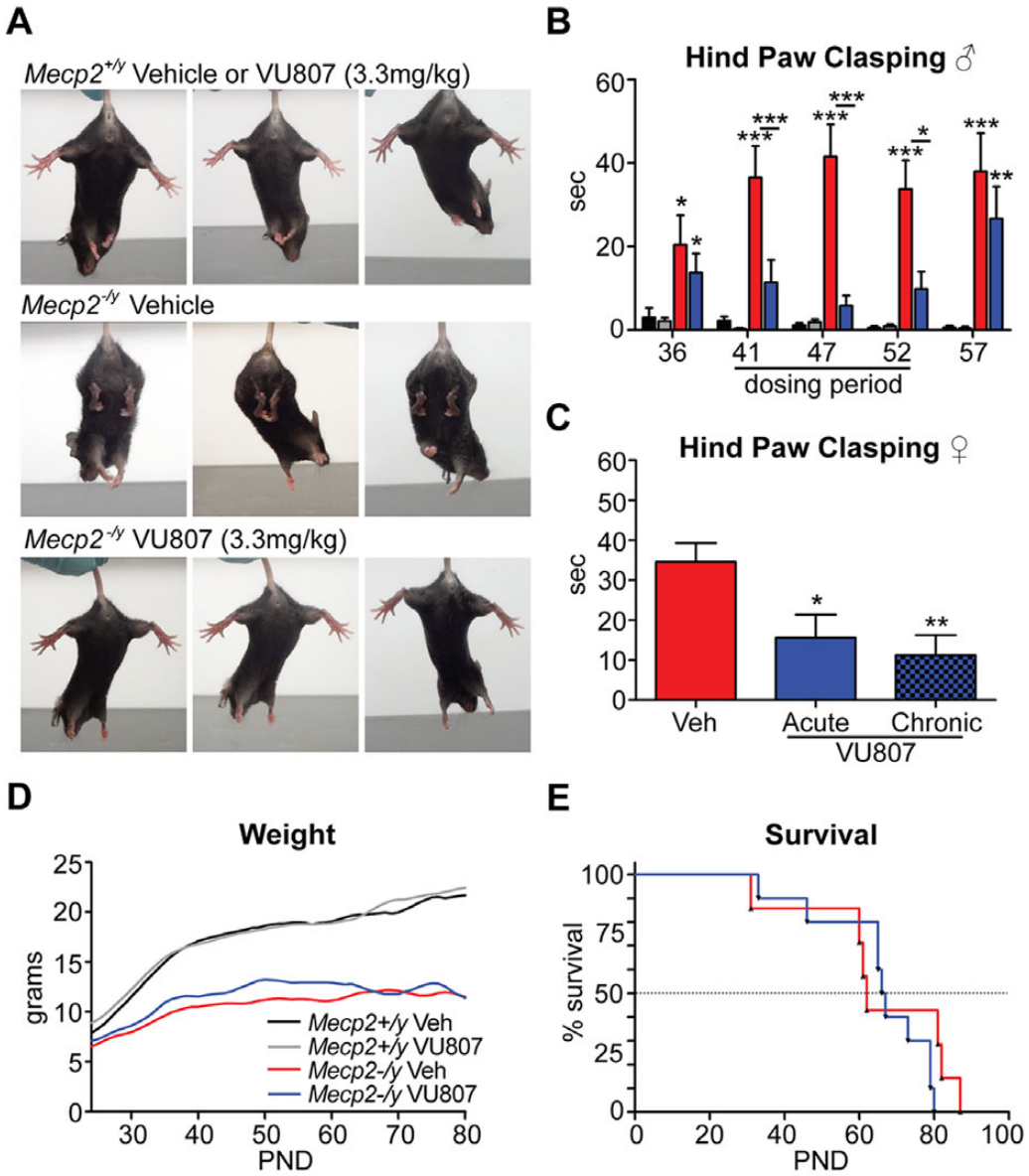


**Figure 5.** VU0462807 (VU807) normalizes hind-paw clasping but fails to rescue survival. (**A**) Representative images of *Mecp2*$^{+/y}$ and *Mecp2*$^{-/y}$ mice treated with 3.3 mg/kg VU807 (IP). $mGlu_5$ PAM treatment ameliorated the clasping phenotype observed in vehicle-treated *Mecp2*$^{-/y}$ animals. (**B**) During the pre-treatment phase, clasping was evident in both vehicle (red, $N = 8$) and VU807 (blue, $N = 7$) treatment groups of *Mecp2*$^{-/y}$ mice. During the 17-day chronic dosing paradigm (QD dosing), VU807 significantly tempered the clasping phenotype at all three time-points tested relative to vehicle-treated *Mecp2*$^{-/y}$ mice (avg.: 37.5 ± 7.4 s/min veh. versus 9.0 ± 4.0 s/min VU0807, $^{**}P \leq 0.01$). Importantly, the clasping phenotype returned in drug-treated mice after dosing was stopped (38.0 ± 9.1 s/min veh. versus 26.7 ± 7.7 s/min VU807), indicating that the benefit is mediated by VU807. *Mecp2*$^{+/y}$ vehicle = Black ($N = 9$), *Mecp2*$^{+/y}$ vehicle = Gray ($N = 8$). Two-way ANOVA, with Bonferroni post-test. (**C**) Hind-paw clasping was also ameliorated in 10–15-week-old female Rett mice (*Mecp2*$^{+/-}$) with 3.3 mg/kg VU807 treatment (IP). *Mecp2*$^{+/-}$ mice were prescreened for clasping as criteria for inclusion. Vehicle-treated mice clasped an average of 34.6 s/min when suspended by their tails. This was significantly reduced to 15.6 s ($^{*}P \leq 0.05$) with acute treatment and 11.3 s/min ($^{**}P \leq 0.01$) with QD dosing for 5 days. $N = 12$, one-way ANOVA with Bonferroni post-test. (**D** and **E**) Relative to vehicle-treated *Mecp2*$^{-/y}$ mice (red), neither weight nor survival was significantly modified by IP, QD dosing of 3.3 mg/kg VU807 (blue) from P21 until death (smoothed curve fit analysis).

As hind-limb clasping is thought to be analogous to hand wringing in human patients, we next sought to validate this potentially translatable endpoint in female RS mice (*Mecp2*$^{+/-}$), which better models the molecular aspects of RS due to their mosaic expression of the mutant *Mecp2* allele. However, as a consequence of random X-chromosome-inactivation, not all female RS mice present with the same phenotypic severity; therefore, a prescreen for inclusion was necessary to identify a population in which clasping was prevalent. The criteria for inclusion were >10 s spent clasping in 10–15-week-old *Mecp2*$^{+/-}$ mice when suspended by the tail for 1 min. A cohort of 24 *Mecp2*$^{+/-}$ mice meeting these criteria was then divided at random into two groups and treated IP, QD with either 3.3 mg/kg VU0462807 or vehicle. Fifteen minutes following the final dose, the mice were suspended by their tail, and their hind-limb dynamics were recorded for 1 min and then scored by a blinded reviewer. Additionally, to explore the effects of chronic dosing, VU0462807-treated mice were also recorded after 5 days of QD dosing. Following repeat

dosing, vehicle-treated *Mecp2*$^{+/-}$ mice clasped for an average of 34.6 ± 4.7 s/min, which was significantly improved to 15.6 ± 5.8 s/min ($P \leq 0.05$) in mice treated acutely with 3.3 mg/kg VU0462807 and 11.3 ± 5.0 s/min ($P \leq 0.01$) in chronically treated mice (Fig. 5C). These results indicate that our reported improvements in hind-limb clasping are preserved with chronic dosing, and are also conserved between models of face (*Mecp2*$^{-/y}$) and construct (*Mecp2*$^{+/-}$) validity.

### VU0462807 does not improve survival in RS mice

To determine VU0462807's effects on weight and survival, *Mecp2*$^{-/y}$ and *Mecp2*$^{+/y}$ mice were dosed IP, QD, with either 3.3 mg/kg VU0462807 or vehicle from P24 until functional death endpoints were reached. A modest weight benefit was observed at advanced stages with VU0462807 treatment (P39–P65), but dissipated to vehicle-treated levels as terminal stages approached (Fig. 5D). Median survival in vehicle-treated *Mecp2*$^{-/y}$ mice was 62.0 days and was 66.5 days in $mGlu_5$ PAM-treated *Mecp2*$^{-/y}$ mice, which failed to reach statistical significance (Fig. 5E). An advanced stage P39–P54 dosing window was also examined; however, the results were identical to P24-FD dosing (Supplementary Material, Fig. S7), suggesting that neither early nor late $mGlu_5$ PAMs treatment benefits weight or survival. Brain weight and body length in *Mecp2*$^{-/y}$ mice were also observed to be significantly reduced, but unaltered by compound treatment (Supplementary Material, Fig. S7).

### The AKT/mTOR/S6K signaling pathway is positively modified by VU0462807

Our initial hypothesis was that $mGlu_5$ PAMs would normalize protein synthesis-dependent synaptic plasticity in RS. To test this hypothesis, we first assessed this parameter in advanced stage *Mecp2*$^{-/y}$ mice (P50–60) using the well-established paradigm of DHPG-induced LTD at the SC-CA1 synapse (17). In brain slices from control *Mecp2*$^{+/y}$ mice, treatment with 100 μM DHPG induced an LTD response that was 46.2 ± 5.1% of the baseline at 60 min following washout (Fig. 6A, black symbols). VU0462807 treatment had no effect on DHPG-induced LTD in slices from control mice, indicating a saturated response to this concentration of DHPG in *Mecp2*$^{+/y}$ animals (40.1 ± 18.0%, gray symbols). Interestingly, VU0462807 did increase fEPSP slope in *Mecp2*$^{+/y}$ mice prior to DHPG treatment, but not in *Mecp2*$^{-/y}$ mice. The mechanism underlying this response is currently unknown; however, it should be noted that pretreatment changes in fEPSP are not unique to VU0462807, as comparable results have also been reported with the structurally distinct $mGlu_5$ PAMs VU0092273 (59) and VU0409551 (39). In contrast to brain slices from *Mecp2*$^{+/y}$ mice, LTD assessed 60 min post DHPG application was absent in slices from *Mecp2*$^{-/y}$ mice (102 ± 1.5%, red symbols), suggestive of a deficit in this form of PSDSP (Fig. 6A). In support of our hypothesis, pre-treatment of slices with 30 μM VU0462807 rescued attenuated LTD, and evoked a response that was 63.8 ± 6.0% of baseline at 60 min post DHPG addition (Fig. 6A, blue symbols).

Building on this finding, we pre-treated *Mecp2*$^{-/y}$ brain slices with 20 nM rapamycin to confirm that this evoked LTD response was due, in part, to normalization of AKT/mTOR signaling. In support of mTOR-mediated LTD, pre-treatment with rapamycin blocked the ability of VU0462807 to potentiate LTD at the SC-CA1 synapse of *Mecp2*$^{-/y}$ hippocampal slices, and the response returned to 90.7 ± 3.4% of the baseline at 60 min post DHPG addition (Fig. 6B, yellow symbols). It is of note that our preliminary studies identified that attenuated LTD in brain slices from *Mecp2*$^{-/y}$ mice was unique to advanced stages of disease (Fig. 6C, red symbols), which we identified as the presence of persistent clasping when suspended by the tail. Mice that were tested prior to this point (P34) presented with an LTD response that was 55.1 ± 5.0% of the baseline (purple symbols), a response that was not statistically different than WT controls at this age (51.6 ± 3.8%, $P \geq 0.05$, not shown graphically). This supports the theory that early- and late-stage RS model mice and patients may have unique therapeutic requirements at different stages of disease progression, which merit consideration during therapeutics development.

Well-characterized electrophysiological methods of assessing PSDSP in the cortex are lacking; however, given recent reports of decreased global protein synthesis in cortical embryonic stem cells from RS mice (12), we chose to examine $mGlu_5$/AKT/mTOR/S6K signaling in the cortex of advanced stage *Mecp2*$^{-/y}$ mice via fluorescent western blotting (Odyssey). *Mecp2*$^{+/y}$ and *Mecp2*$^{-/y}$ mice were dosed with either vehicle or VU0462807 IP, QD from P39 to P54 and brain tissue was harvested exactly 30 min following the final dose on P54. A 30 min time-point was chosen to allow 15 min for the compound to reach $C_{max}$ and 15 min for downstream signaling to occur. To survey for sustained benefits after the compound had cleared, brain samples from one additional group of VU0462807-treated mice were harvested 24 h following the final dose. As has been demonstrated in other studies (13), we observed a significant decrease in the ratio of phosphorylated to total (P/T) AKT, mTOR and S6K in the cortex of vehicle-treated *Mecp2*$^{-/y}$ mice (Fig. 6D and E). VU0462807 treatment significantly increased the P/T ratio of these proteins both 30 min and 24 h after the final dose was given, indicative of normalized $mGlu_5$/AKT/mTOR/S6K signaling.

## Discussion

$mGlu_5$ allosteric modulation has been proposed as an effective means of normalizing E–I imbalance in Autism Spectrum Disorders, including RS. Here, we report decreased *GRM5* gene expression in several regions of the *Mecp2*$^{-/y}$ mouse brain and in the motor cortex of RS autopsy samples. Furthermore, we show that treatment with our novel $mGlu_5$ PAM improves motor phenotypes, cued fear conditioning and hind-paw clasping. Additionally, we have demonstrated that attenuated LTD and decreased AKT/S6K signaling can be corrected by VU0462807 treatment, suggesting that the reported phenotypic improvements also correlated with the proposed mechanism of normalized protein synthesis-dependent synaptic plasticity. Importantly, VU0462807 improved these phenotypes without evoking any overt adverse effects in a highly vulnerable disease context. This result provides strong credence to the potential utility of $mGlu_5$ PAMs in the treatment of ASDs, and for the potential to develop $mGlu_5$ PAMs that are devoid of adverse effects (38,39).

In many ways, the symptomatology of RS epitomizes the challenges associated with $mGlu_5$ PAM drug development. On one hand, aspects of the disease appear to be an ideal fit for $mGlu_5$ positive modulation as they are characterized by synaptic plasticity defects consistent with reductions in $mGlu_5$ activity (12,13). Conversely, the robust penetrance of seizures in this patient population suggests that the target's largest adverse effect liability is at risk of exacerbating the etiology of the disease. Unfortunately, this situation is not unique to RS, as other proposed indications for $mGlu_5$ modulation, such as TSC1 and schizophrenia, also present with increased seizure susceptibility as a normal aspect of disease progression (60–62) and have the same liability for adverse effects. Furthermore, episodes of breath

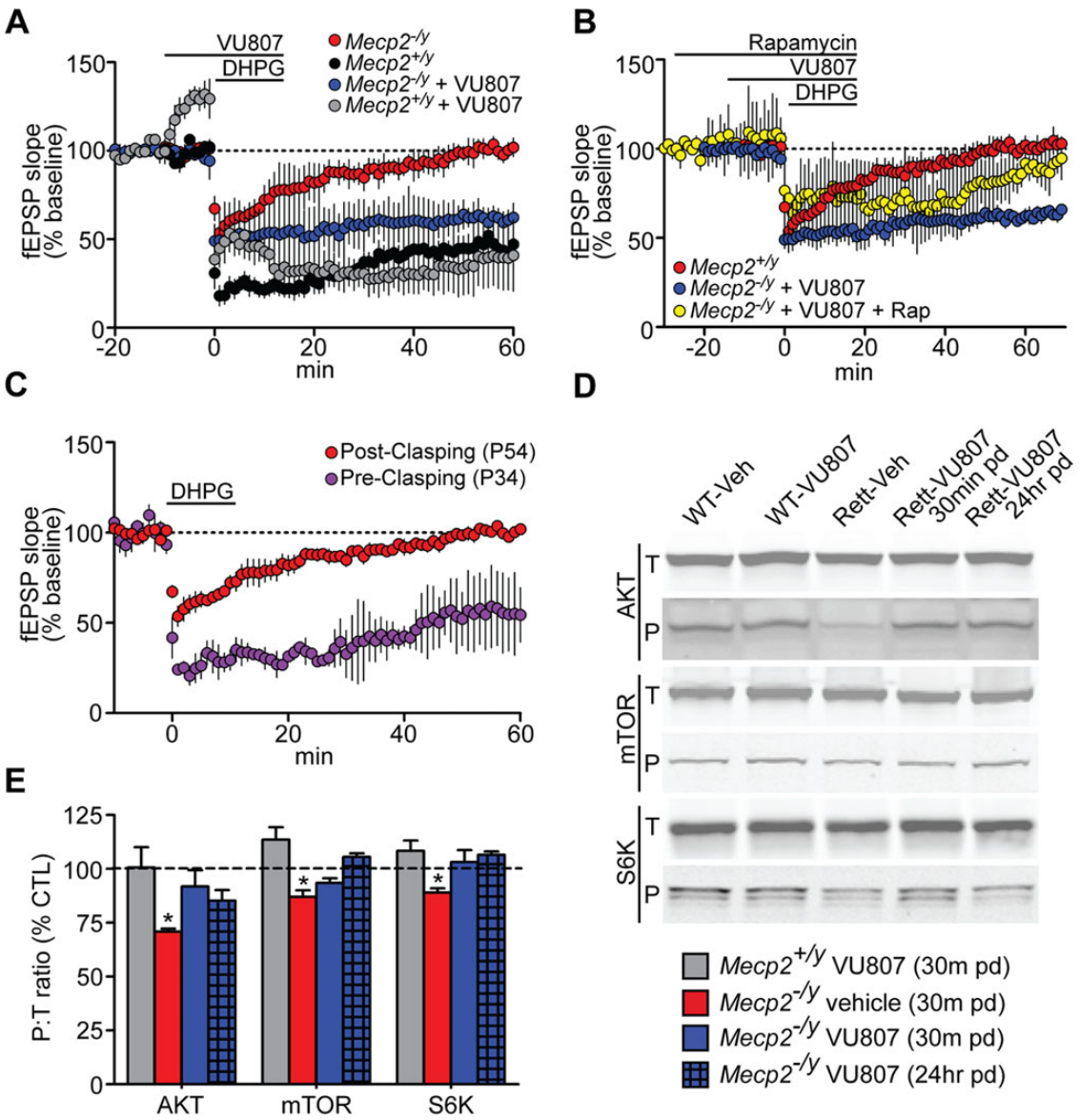


**Figure 6.** Protein synthesis-dependent forms of synaptic plasticity are normalized by VU0462807 (VU807). (**A**) DHPG (100 μM)-induced LTD at the SC-CA1 synapse was attenuated in P50–60 *Mecp2*$^{-/y}$ mice (red) 60 min following washout of drug (102 ± 1.5% of baseline), whereas slices from *Mecp2*$^{+/y}$ mice demonstrated a robust LTD response (46.2 ± 5.1% of baseline, $N = 4$) (black). Pretreatment with 30 μM VU807 potentiated attenuated LTD in *Mecp2*$^{-/y}$ mice to 63.8 ± 6.0% (blue)($N = 4$, $^{***}P \leq 0.001$ relative to DHPG alone in *Mecp2*$^{-/y}$ slices, Student's *t*-test). (**B**) VU807's ability to potentiate attenuate LTD at the SC-CA1 synapse was lost when slices were pretreated with 20 nM rapamycin (yellow, 90.7 ± 3.4% at 60 min, $N = 4$). (**C**) DHPG-induced LTD was only attenuated in *Mecp2*$^{-/y}$ mice that consistently presented with hind-paw clasping phenotypes. Prior to this point, DHPG was able to induce an LTD response in slices that was comparable to controls (purple, 55.1 ± 5.0% of the baseline ($N = 5$). (**D–E**) Odyssey western blotting of the ratio between phosphorylated and total AKT (Ser$^{473}$), mTOR (Ser$^{2448}$) and S6K (Thr$^{421}$). P54 vehicle-treated *Mecp2*$^{-/y}$ mice exhibited significant reductions in the ratio of P:T AKT (70.8 ± 1.4%, $^{*}P \leq 0.05$), mTOR (87.0 ± 3.0%, $^{*}P \leq 0.05$) and S6K (89.0 ± 2.0%, $^{*}P \leq 0.05$) relative to vehicle-treated *Mecp2*$^{+/y}$ controls (100%, dashed black line). pd = post dose. Student's *t*-test, $N \geq 6$/treatment group. Data represent mean ± SEM.

holding or apneas in RS are believed to originate from hyperactivity of respiratory circuits in the brain stem (63), resulting in the inherent risk of intensifying this phenotype by increasing glutamatergic tone via $mGlu_5$. At the molecular level, it is worth noting that interventions such as TrkB agonists, IGF-1 peptides and $mGlu_5$ PAMs all are believed to positively upregulate AKT signaling, and all provide some degree of phenotypic rescue to motor systems (26,27,64). However, unlike strategies that target pleiotropic growth factors, VU0462807 did not extend survival in *Mecp2*$^{-/y}$ mice. It is unclear if this result was due to a lack of 24 h VU0462807 exposure, or whether it is indicative that the survival benefits observed with growth factor mimetic strategies are autonomous from the AKT/mTOR/S6K signaling pathway. Further work with both classes of compounds will be important to determine which is the case, and whether co-administration has additive therapeutic value.

In contrast to what we have observed with metabotropic glutamate receptor modulation, compounds that decrease inotropic Glu (iGlu) function, such as the NMDAR antagonists ketamine and AZD6765, have been reported to normalize macrocircuits in the *Mecp2*-deficient rodent brain, including those responsible for respiratory dysfunction (65). On the surface, our $mGlu_5$ PAM data may appear to conflict with data observed with NMDAR antagonists, since both are glutamate receptors and modulate each

other in a complex fashion. However, the finding that $mGlu_5$ PAMs can be optimized to display stimulus bias and not potentiate NMDAR currents or NMDA-dependent forms of synaptic plasticity raises the possibility that potentiation of $mGlu_5$ signaling, without enhancing NMDAR currents, could provide efficacy without the potential liabilities of excessive NMDAR signaling.

One critical discrepancy between our studies and those of others is that of attenuated DHPG-induced LTD at the SC-CA1 synapse in RS mice. In a set of analogous studies, Moretti *et al.* (6) demonstrated that DHPG-induced LTD was indistinguishable from controls in 4–7-week-old mice harboring a stop-codon downstream of amino acid 308 ($Mecp2^{308/y}$), which is in direct opposition to our finding of attenuated DHPG-LTD in 7–8-week-old $Mecp2^{tm1.1Bird/y}$ mice. However, when coupled with the fact that $Mecp2^{308/y}$ mice do not present with a robust phenotype at 4–7 weeks of age, our observation that LTD is not attenuated until post-symptomatic time-points provides an explanation for this discrepancy. The co-appearance of synaptic plasticity defects and overt symptoms is not unique to DHPG-LTD, as our work shares many parallels with the study by Weng *et al.* (66), in which high-frequency stimulation-induced LTP and post-tetanic potentiation were only abated in post-symptomatic $Mecp2^{-/y}$ mice. When these advanced-stage findings are placed in context with the defects in synaptogenesis observed in *Mecp2*-deficient mice, it becomes apparent that RS is, at least, a biphasic disease. This contention is supported by the progression of the disease in patients, with developmental regression occurring rapidly over a period of months, and advanced-stage RS progressing slowly over a period of decades. Such a divergence between the etiologies of early and late state RS will merit careful considerations throughout the therapeutic development process, as inappropriate timing could impact the efficacy and adverse effect liability of therapeutic strategies depending upon the stage of intervention. Here, we have demonstrated that $mGlu_5$ positive modulation improves advanced stage RS phenotypes. While this represents an exciting discovery, future work will be required to determine the extent to which this is true at all phases of disease.

## Materials and Methods

### Mouse model

Primary screening for convulsive adverse effects was performed in male WT congenic *FVB/N* mice (Jackson Labs #001800), aged 6 weeks. The RS mouse model used was generated by breeding a C57Bl/6 congenic male mouse (Jackson Labs #000664) with a $Mecp2^{+/tm1.1bird}$ female also on a congenic C57Bl/6 background (Jackson Labs #003890). Fluid and nutrient support in the form of Clear H2O 76A diet gel packs were provided to nursing mothers and pups from P10 to P21, and to advanced-stage male mutants and controls until the time of their death. Note that if nutrient support was provided pre-weaning, 100% of the pups survived to adult ages. Consistent with Vanderbilt IAUCUC protocols functional death endpoints were used instead of terminal endpoints. Functional death was defined as three consecutive days of weight loss averaging >0.5 g/day, dramatic loss in motor function and/or pronounced lethargy.

### Cell culture and calcium mobilization assays

HEK293A cells stably expressing rat $mGlu_5$ were maintained and measurement of $mGlu_5$-mediated intracellular $Ca^{2+}$ mobilization was performed as previously described (38,41,67). For selectivity screening, calcium flux in HEK293 cells stably expressing rat $mGlu_1$ or thallium flux through GIRK channels in HEK-293-GIRK cells expressing mGlu subtypes 2, 3, 4, 6, 7 or 8 (all rat isoforms with the exception of $mGlu_6$, which was human) was measured as described in Supplementary Material, Experimental Procedures (41,67,68). Control (#01279-107.NC001) and *MECP2*-deficient (#01279.730) iPSCs were gifted from Cellular Dynamics International, and cultured in accordance with manufacturer's instructions.

### Drug metabolism and pharmacokinetics

The *in vitro* and *in vivo* rat drug metabolism and pharmacokinetic properties of VU0462807 were determined as previously described (69–71) in male SD rats and C57/B6 mice.

### Amphetamine-induced hyperlocomotion

Effects of VU0462807 on amphetamine-induced hyperlocomotion were determined as previously described (41). Briefly, male SD rats were placed in an open-field chamber (KinderScientific, San Diego, CA) for 60 min. At t = 25, 30 rats were administered vehicle or VU0462807 (0.3–30 mg/kg, p.o., 20% β-cyclodextrin in water, 10 ml/kg, N = 8) followed by amphetamine (1 mg/kg, s.c., saline, 1 ml/kg) at t = 60 min. Locomotor activity was measured for an additional 60 min. Changes in locomotor activity were measured as the total number of photobeam breaks per 5 min bins. Data are expressed as mean ± SEM and analyzed using one-way ANOVA (60–120 min) with a Dunnett's *post hoc* test comparing all dosing groups to vehicle + amphetamine-treated controls. Statistical significance was determined as $P < 0.05$.

### Extracellular field potential recordings

Transverse hippocampal slices were prepared from young adult (P29–P36) male SD rats (Charles River, Wilmington, MA) in compound characterization studies and in P50–P60 and P34 $Mecp2^{tm1.1bird}$ line mice, with use of standard techniques and buffers as previously described (15,59). In brief, a bipolar-stimulating electrode was placed in the stratum radiatum near the CA3–CA1 border to stimulate the Schaffer collaterals and field potential recordings were acquired from the stratum radiatum of area CA1. $mGlu_5$ compounds were diluted to the appropriate concentrations in dimethylsulfoxide (0.1% final) in aCSF and applied to the bath for 10–20 min with use of a perfusion system. Chemically-induced mGlu LTD was initiated by the application of DHPG in aCSF (25 or 75 μM rat, 100 μM mice) for 10 min. For mTOR-dependent LTD studies, 20 nM rapamycin was applied 30 min prior to DHPG. Threshold LTP was induced by one train of theta burst stimulation (TBS; nine bursts of four pluses at 100 Hz, 230 ms interburst interval). Saturated LTP was induced by four trains of 10 Hz TBS (nine bursts of four pulses at 100 Hz, 100 ms interburst interval). Data were analyzed using Clampfit 10.2 and GraphPad Prism 5.0 as described previously (15,59). Between-group statistics were performed using one-way analysis of variance (ANOVA) and for within-group analysis repeated measures ANOVA was performed (*P*-value of <0.05 considered significant). Multiple comparisons were performed using Dunnett's multiple comparison test for comparing with a control group ($P < 0.05$ considered significant).

### Expression studies

#### *Quantitative real-time PCR*

Cortex (total and motor), hippocampus and striatum were microdissected from P10, P30 and P50 ± 2-day-old $Mecp2^{-/y}$ and $Mecp2^{+/y}$

mice on a C57/B6 congenic background (N = 5/genotype). Samples were homogenized with a mortar and pestle and total RNA was prepared using Trizol Reagent® (Life Technologies) in accordance with manufacturer's instructions. Total RNA from each brain region was DNase-treated with Roche Turbo DNase™ kit, and cDNA from 2 µg total RNA was synthesized using the Superscript Variable Input Linear Output (VILO™) kit (Invitrogen). QRT-PCR on cDNA from 25 ng of initial RNA template was then run in triplicate using Taqman Fast Reagent Mix® (Life Technologies) and a Life Technologies gene expression assay for *Grm5* (Mm0069332_m1). Cycle threshold (Ct) values for each sample were normalized to *Gapdh* (Mm03302249_g1) expression and analyzed using the delta–delta Ct method. Values exceeding two times the standard deviation were classified as outliers and removed. Each value was compared with the average delta-Ct of the $Mecp2^{+/y}$ mice and calculated as percent-relative to the average control delta-Ct. Statistical analysis compared $Mecp2^{-/y}$ and $Mecp2^{+/y}$ expression in each brain regions using a Student's *t*-test.

Western blots were performed using standard quantitative fluorescent western blotting techniques (Odyssey). Fifty micrograms of total protein was loaded for AKT blots and 25 µg for $mGlu_5$, $ERK_{1/2}$, mTOR and S6K blots. Antibodies were diluted in Odyssey block (LiCor #927-40000) and used at the following concentrations: $mGlu_5$ (Millipore #AB5675, 1:1000); AKT [Cell Signaling (CS) #9272, 1:1000]; P-AKT-$Ser^{473}$ (CS #4051, 1:1000); $ERK_{1/2}$ (CS #9102s, 1:1000); P-$ERK_{1/2}$ $Thr^{202/}Tyr^{204}$ (CS #9106l,1:1000); mTOR (CS #4217, 1:1000); P-mTor-$Ser^{2448}$ (CS #2971, 1:1000); S6K (Santa Cruz # 8418, 1:1000); P-S6K-$Thr^{421}$/$Ser^{424}$ (CS #9204, 1:1000); TrkB (CS #4603, 1:1000); P-TrkB-$Try^{817}$ (Abcam, 1:1000); Tubulin (E7, DHB, 1:4000); Goat Anti-Mouse 680 (LiCor # 926-68020, 1:5000); Goat Anti-Rabbit 800 (LiCor #926-32211, 1:5000).

#### *Seizure phenotyping*

Six-week-old FVBN male mice were dosed (IP) with the $mGlu_5$ PAMs VU0361747 (10 mg/kg), VU0462807 (10 mg/kg), CDPPB (10 mg/kg), the $mGlu_5$ allosteric agonist VU0424465 (1 mg/kg) and vehicle (10% Tween 80 in water) (N = 5/compound). Mice were then given a score based on a Racine Scale once every 5 min over the span of 1 h, with the scorer blinded to the treatment group. The Racine score used was as follows: 1 = mouth and/or facial movements, increased digging; 2 = head nodding; 3 = forelimb clonus and tonic tail; 4 = rearing and/or tonic body; 5 = generalized seizure with motor convulsions. For studies in $Mecp2^{tm1.1bird}$ mice, 3.3 mg/kg VU0462807 or vehicle (10% Tween 80 in water) was dosed one time daily from P39 until P54. Racine scores were given on P39 and P54 as described for FVBN mice to represent acute and chronic compound administration.

#### *Pulse oximetry*

To investigate cardiorespiratory phenotypes, pulse oximetry was used (Mouse Ox). Twenty-four hours prior to the assay, the neck hair of the mice was removed using NAIR™. Hair removal cream was applied in 1 min increments until hair was fully gone, wiped with a paper towel and then washed with cold $H_2O$. Mice were then given 24 h to recover in their home cage. On the day of the assay, mice were fitted with a dummy collar for a period of 2 h prior to testing. At the time of the test, the sham collar was replaced with a recording collar, the mouse was then injected IP with 3.3 mg/kg VU0462807 or vehicle (10% Tween 80 in water), and then allowed to acclimate to the recording chamber for a period of 10 min. Ten minutes of motionless recording was acquired using the Mouse Ox software, with the acquisition averaging rate dropped from 5× to 1×. This provided core breath rate, heart rate and pulse distention values. Breath-rate charts were then de-identified and quantified by a blinded reviewer to quantify periods where the breath rate dropped significantly.

#### *Conditioned fear*

Conditioned fear was utilized as a measure of hippocampal and amygdala function. 48 and 24 h prior to the test, mice were allowed to acclimate to the testing room for 1–2 h. On the day of the test, the mice were allowed to acclimate to the room for 1 h prior to the assay. Mice were then injected IP with either 3.3 mg/kg of VU0462807 or vehicle. At $T_{max}$ of the compound, mice were placed into the tone-shock chamber. The training paradigm used was 3 min of acclimation, 1–30 s tone followed by a 0.7 mA shock, a 30 s consolidation period, followed by a second tone-shock pairing. Mice that were immobile for >30% of the pre-shock habituation/acclimation phase were deemed to have motor impairments that could be misinterpreted as freezing, and were removed from the study. Twenty-four hours after training, the mice were reintroduced into the same chamber for a period of 4 min to quantify contextual fear conditioning. Approximately 1 h following the contextual assay, mice were placed into a novel apparatus containing a 10% almond scent, where a tone was played for a period of 1 min. In each case, the percent of time spent freezing was used as an outcome measure.

#### *Open-field*

To conduct the open-field assay, mice were injected IP with 3.3 mg/kg VU0462807 or vehicle (10% Tween 80 in water) and placed in the activity chamber. Exploratory and locomotor behavior was then monitored using Activity software to quantify beam breaks in the X, Y and Z over the course of the 60 min test.

#### *High-speed ventral plane videography*

Assessments of gait dynamics of $Mecp2^{+/y}$ and $Mecp2^{-/y}$ mice were made using the Treadscan system of gait analysis. Mice were first run untreated at P35 to establish (i) that they were capable of completing the assay and (ii) a baseline value for gait function. Mice were then injected IP with 3.3 mg/kg VU0462807 or vehicle (10% Tween 80) daily from P39 to 54, with the compound de-identified for blinding purposes. Two training runs were conducted on P39 and P46, with the quantified test occurring on P54. An untreated post-test was also run on P59. Tests occurred at $T_{max}$ of the compound (15 min) and occurred for a period of 30 s of continuous running. Discrete video clips of fluid gait were identified by the Treadscan software and then manually culled to eliminate video clips where lateral movement was observed. Software paw ID training modules were built from $Mecp2^{-/y}$ mice and used to process gait dynamics in accordance with the manufacturer's instructions.

### Survival studies

To determine whether our novel $mGlu_5$ PAM extended survival, mice were dosed (IP, QD) with 3.3 mg/kg VU0462807 or vehicle (10% Tween 80 in water) from P21 until death or P39–P54. Functional death endpoints were used, which were defined as three consecutive days of >0.5 g weight loss, gross functional decline and/or severe lethargy. Weights were recorded once daily.

### Hind-paw clasping

To quantify hind-paw clasping, mice were suspended by their tail for a period of 1 min. Their hind-limb dynamics were recorded on video and analyzed by a blinded reviewer. Recording occurred at $T_{max}$ of the compound (15 min) in mice that were treated (IP) with VU0462807 (3.3 mg/kg) or vehicle (10% Tween 80) from P39 to P54 in male and for 5 days in 10–15-week-old clasping females. Clasping was defined as the number of seconds spent either clasping

one or more paws, or knuckling the digits of the paw. Mice were returned to their home cage for the time period between dosing and assessment. In males, the assay was conducted prior to treatment on Day P36, during treatment on Days P41, P47, P52 and post-treatment on Day P57. In females, mice were dosed for five consecutive days with either VU0462807 or vehicle and assessed on the first (acute) and last (chronic) day of dosing. On the day the assay was conducted, the mice being tested underwent no other phenotypic assays.

## Supplementary Material

Supplementary Material is available at *HMG* online.

## Acknowledgements

VU0462807 was developed as part of a collaboration between the Vanderbilt Center For Neuroscience Drug Discovery, Johnson & Johnson and Janssen Pharmaceuticals. IPSC cells were obtained through a collaborative effort with Cellular Dynamics International. Control and Rett syndrome autopsy samples were a generous gift facilitated by Rettsyndrome.org. Specifically, control human tissue was obtained from the University of Maryland Brain and Tissue Bank, which is a brain and tissue repository of the NIH NeuroBioBank. Rett Syndrome samples were provided by the Harvard Brain Tissue Resource Center, which is supported in part by PHS contract, HHSN-271-3013-00030C (NIMH, NINDS and NICHD). We would also like to acknowledge the contribution of Samantha Kopinsky in the processing of gait videos.

*Conflict of Interest statement*. C.M.N., C.K.J., C.W.L. and J.S.D. have received research funding and royalties from Johnson & Johnson, AstraZeneca, Bristol-Myers Squibb, the Michael J. Fox Foundation and Seaside Therapeutics. C.K.J. is also funded by the Autism Speaks PACT consortium. P.J.C. has received research funding and royalties from Johnson & Johnson, AstraZeneca, Bristol-Myers Squibb, Michael J Fox Foundation and Seaside Therapeutics. Over the past 3 years he has consulted for Pfizer, Cambridge, and has served on the Scientific Advisory Boards of Seaside Therapeutics, Michael J. Fox Foundation, Stanley Center for Psychiatric Research Broad Institute (MIT/Harvard), Karuna Pharmaceuticals, Lieber Institute for Brain Development Johns Hopkins University, Clinical Mechanism (POCM) and Proof of Concept (POC) Consortium and Neurobiology Foundation for Schizophrenia and Bipolar Disorder. The remaining authors have no conflicts of interest.

## Funding

This work was supported by a Treatment Award from Autism Speaks to C.M.N., National Institutes of Health grants: (R21 MH102548) to C.M.N. and (R01 NS031373) to P.J.C., and a Basic Research grant from Rettsyndrome.org to C.M.N. R.G.G. was supported by a mentored training fellowship from Rettsyndrome.org, R.K.S. was supported by a Weatherstone Predoctoral Fellowship from Autism Speaks and the Howard Hughes Medical Institute Certificate Program in Molecular Medicine (HHMI CPMM) through Vanderbilt University. A.G.W. was supported by a postdoctoral fellowship through the Pharmaceutical Research and Manufacturers of America (PhRMA) Foundation.

## References

1. Amir, R.E., Van den Veyver, I.B., Wan, M., Tran, C.Q., Francke, U. and Zoghbi, H.Y. (1999) Rett syndrome is caused by mutations in X-linked MECP2, encoding methyl-CpG-binding protein 2. *Nat. Genet.*, **23**, 185–188.
2. Nomura, Y. and Segawa, M. (2005) Natural history of Rett syndrome. *J. Child Neurol.*, **20**, 764–768.
3. Asaka, Y., Jugloff, D.G., Zhang, L., Eubanks, J.H. and Fitzsimonds, R.M. (2006) Hippocampal synaptic plasticity is impaired in the Mecp2-null mouse model of Rett syndrome. *Neurobiol. Disease*, **21**, 217–227.
4. Chen, R.Z., Akbarian, S., Tudor, M. and Jaenisch, R. (2001) Deficiency of methyl-CpG binding protein-2 in CNS neurons results in a Rett-like phenotype in mice. *Nat. Genet.*, **27**, 327–331.
5. Guy, J., Hendrich, B., Holmes, M., Martin, J.E. and Bird, A. (2001) A mouse Mecp2-null mutation causes neurological symptoms that mimic Rett syndrome. *Nat. Genet.*, **27**, 322–326.
6. Moretti, P., Levenson, J.M., Battaglia, F., Atkinson, R., Teague, R., Antalffy, B., Armstrong, D., Arancio, O., Sweatt, J.D. and Zoghbi, H.Y. (2006) Learning and memory and synaptic plasticity are impaired in a mouse model of Rett syndrome. *J. Neurosci. Official J. Soc. Neurosci.*, **26**, 319–327.
7. Pelka, G.J., Watson, C.M., Radziewic, T., Hayward, M., Lahooti, H., Christodoulou, J. and Tam, P.P. (2006) Mecp2 deficiency is associated with learning and cognitive deficits and altered gene activity in the hippocampal region of mice. *Brain: J. Neurol.*, **129**, 887–898.
8. Shahbazian, M., Young, J., Yuva-Paylor, L., Spencer, C., Antalffy, B., Noebels, J., Armstrong, D., Paylor, R. and Zoghbi, H. (2002) Mice with truncated MeCP2 recapitulate many Rett syndrome features and display hyperacetylation of histone H3. *Neuron*, **35**, 243–254.
9. Maliszewska-Cyna, E., Bawa, D. and Eubanks, J.H. (2010) Diminished prevalence but preserved synaptic distribution of N-methyl-D-aspartate receptor subunits in the methyl CpG binding protein 2(MeCP2)-null mouse brain. *Neuroscience*, **168**, 624–632.
10. Nguyen, M.V., Du, F., Felice, C.A., Shan, X., Nigam, A., Mandel, G., Robinson, J.K. and Ballas, N. (2012) MeCP2 is critical for maintaining mature neuronal networks and global brain anatomy during late stages of postnatal brain development and in the mature adult brain. *J. Neurosci. Official J. Soc. Neurosci.*, **32**, 10021–10034.
11. Zhong, X., Li, H. and Chang, Q. (2012) MeCP2 phosphorylation is required for modulating synaptic scaling through mGluR5. *J. Neurosci. Official J. Soc. Neurosci.*, **32**, 12841–12847.
12. Li, Y., Wang, H., Muffat, J., Cheng, A.W., Orlando, D.A., Loven, J., Kwok, S.M., Feldman, D.A., Bateup, H.S., Gao, Q. *et al.* (2013) Global transcriptional and translational repression in human-embryonic-stem-cell-derived Rett syndrome neurons. *Cell Stem Cell*, **13**, 446–458.
13. Ricciardi, S., Boggio, E.M., Grosso, S., Lonetti, G., Forlani, G., Stefanelli, G., Calcagno, E., Morello, N., Landsberger, N., Biffo, S. *et al.* (2011) Reduced AKT/mTOR signaling and protein synthesis dysregulation in a Rett syndrome animal model. *Hum. Mol. Genet.*, **20**, 1182–1196.
14. Schuman, E.M., Dynes, J.L. and Steward, O. (2006) Synaptic regulation of translation of dendritic mRNAs. *J. Neurosci. Official J. Soc. Neurosci.*, **26**, 7143–7146.
15. Ayala, J.E., Chen, Y., Banko, J.L., Sheffler, D.J., Williams, R., Telk, A.N., Watson, N.L., Xiang, Z., Zhang, Y., Jones, P.J. *et al.* (2009) mGluR5 positive allosteric modulators facilitate both hippocampal LTP and LTD and enhance spatial learning. *Neuropsychopharmacol. Official Pub. Am. Coll. Neuropsychopharmacol.*, **34**, 2057–2071.
16. Bear, M.F., Dolen, G., Osterweil, E. and Nagarajan, N. (2008) Fragile X: translation in action. *Neuropsychopharmacol. Official Pub. Am. Coll. Neuropsychopharmacol.*, **33**, 84–87.

17. Huber, K.M., Kayser, M.S. and Bear, M.F. (2000) Role for rapid dendritic protein synthesis in hippocampal mGluR-dependent long-term depression. *Science*, **288**, 1254–1257.
18. Huber, K.M., Roder, J.C. and Bear, M.F. (2001) Chemical induction of mGluR5- and protein synthesis—dependent long-term depression in hippocampal area CA1. *J. Neurophysiol.*, **86**, 321–325.
19. Piers, T.M., Kim, D.H., Kim, B.C., Regan, P., Whitcomb, D.J. and Cho, K. (2012) Translational concepts of mGluR5 in synaptic diseases of the brain. *Front. Pharmacol.*, **3**, 199.
20. Cracco, J.B., Serrano, P., Moskowitz, S.I., Bergold, P.J. and Sacktor, T.C. (2005) Protein synthesis-dependent LTP in isolated dendrites of CA1 pyramidal cells. *Hippocampus*, **15**, 551–556.
21. Kang, H. and Schuman, E.M. (1996) A requirement for local protein synthesis in neurotrophin-induced hippocampal synaptic plasticity. *Science*, **273**, 1402–1406.
22. Auerbach, B.D., Osterweil, E.K. and Bear, M.F. (2011) Mutations causing syndromic autism define an axis of synaptic pathophysiology. *Nature*, **480**, 63–68.
23. Li, W., Cui, Y., Kushner, S.A., Brown, R.A., Jentsch, J.D., Frankland, P.W., Cannon, T.D. and Silva, A.J. (2005) The HMG-CoA reductase inhibitor lovastatin reverses the learning and attention deficits in a mouse model of neurofibromatosis type 1. *Curr. Biol. CB*, **15**, 1961–1967.
24. Tian, D., Stoppel, L.J., Heynen, A.J., Lindemann, L., Jaeschke, G., Mills, A.A. and Bear, M.F. (2015) Contribution of mGluR5 to pathophysiology in a mouse model of human chromosome 16p11.2 microdeletion. *Nat. Neurosci.*, **18**, 182–184.
25. Jiang, M., Ash, R.T., Baker, S.A., Suter, B., Ferguson, A., Park, J., Rudy, J., Torsky, S.P., Chao, H.T., Zoghbi, H.Y. *et al.* (2013) Dendritic arborization and spine dynamics are abnormal in the mouse model of MECP2 duplication syndrome. *J. Neurosci. Official J. Soc. Neurosci.*, **33**, 19518–19533.
26. Kron, M., Lang, M., Adams, I.T., Sceniak, M., Longo, F. and Katz, D.M. (2014) A BDNF loop-domain mimetic acutely reverses spontaneous apneas and respiratory abnormalities during behavioral arousal in a mouse model of Rett syndrome. *Dis. Model. Mech.*, **7**, 1047–1055.
27. Schmid, D.A., Yang, T., Ogier, M., Adams, I., Mirakhur, Y., Wang, Q., Massa, S.M., Longo, F.M. and Katz, D.M. (2012) A TrkB small molecule partial agonist rescues TrkB phosphorylation deficits and improves respiratory function in a mouse model of Rett syndrome. *J. Neurosci. Official J. Soc. Neurosci.*, **32**, 1803–1810.
28. Tropea, D., Giacometti, E., Wilson, N.R., Beard, C., McCurry, C., Fu, D.D., Flannery, R., Jaenisch, R. and Sur, M. (2009) Partial reversal of Rett syndrome-like symptoms in MeCP2 mutant mice. *Proc. Natl Acad. Sci. USA*, **106**, 2029–2034.
29. Xu, L., Zhang, Y., Cohen, S.B. and DiPetrillo, K. (2010) TrkB agonist antibody dose-dependently raises blood pressure in mice with diet-induced obesity. *Am. J. Hypertens.*, **23**, 732–736.
30. Niswender, C.M. and Conn, P.J. (2010) Metabotropic glutamate receptors: physiology, pharmacology, and disease. *Ann. Rev. Pharmacol. Toxicol.*, **50**, 295–322.
31. Gallagher, S.M., Daly, C.A., Bear, M.F. and Huber, K.M. (2004) Extracellular signal-regulated protein kinase activation is required for metabotropic glutamate receptor-dependent long-term depression in hippocampal area CA1. *J. Neurosci. Official J. Soc. Neurosci.*, **24**, 4859–4864.
32. Ronesi, J.A. and Huber, K.M. (2008) Homer interactions are necessary for metabotropic glutamate receptor-induced long-term depression and translational activation. *J. Neurosci. Official J. Soc. Neurosci.*, **28**, 543–547.
33. Volk, L.J., Daly, C.A. and Huber, K.M. (2006) Differential roles for group 1 mGluR subtypes in induction and expression of chemically induced hippocampal long-term depression. *J. Neurophysiol.*, **95**, 2427–2438.
34. Bear, M.F. (2005) Therapeutic implications of the mGluR theory of fragile X mental retardation. *Gene. Brain Behav.*, **4**, 393–398.
35. Bear, M.F., Huber, K.M. and Warren, S.T. (2004) The mGluR theory of fragile X mental retardation. *Trend. Neurosci.*, **27**, 370–377.
36. Bhakar, A.L., Dolen, G. and Bear, M.F. (2012) The pathophysiology of fragile X (and what it teaches us about synapses). *Ann. Rev. Neurosci.*, **35**, 417–443.
37. Parmentier-Batteur, S., Hutson, P.H., Menzel, K., Uslaner, J.M., Mattson, B.A., O'Brien, J.A., Magliaro, B.C., Forest, T., Stump, C. A., Tynebor, R.M. *et al.* (2013) Mechanism based neurotoxicity of mGlu5 positive allosteric modulators: development challenges for a promising novel antipsychotic target. *Neuropharmacology*, **82**, 161–173.
38. Rook, J.M., Noetzel, M.J., Pouliot, W.A., Bridges, T.M., Vinson, P.N., Cho, H.P., Zhou, Y., Gogliotti, R.D., Manka, J.T., Gregory, K.J. *et al.* (2012) Unique signaling profiles of positive allosteric modulators of metabotropic glutamate receptor subtype 5 determine differences in *in vivo* activity. *Biol. Psychiatr.*, **6**, 501–509.
39. Rook, J.M., Xiang, Z., Lv, X., Ghoshal, A., Dickerson, J.W., Bridges, T.M., Johnson, K.A., Foster, D.J., Gregory, K.J., Vinson, P.N. *et al.* (2015) Biased mGlu-positive allosteric modulators provide *in vivo* efficacy without potentiating mGlu modulation of NMDAR currents. *Neuron*, **86**, 1029–1040.
40. Malosh, C., Turlington, M., Bridges, T.M., Rook, J.M., Noetzel, M.J., Vinson, P.N., Steckler, T., Lavreysen, H., Mackie, C., Bartolome-Nebreda, J.M. *et al.* (2015) Acyl dihydropyrazolo[1,5-a] pyrimidinones as metabotropic glutamate receptor 5 positive allosteric modulators. *Bioorg. Med. Chem. Lett.*, **25**, 5115–51120.
41. Rodriguez, A.L., Grier, M.D., Jones, C.K., Herman, E.J., Kane, A. S., Smith, R.L., Williams, R., Zhou, Y., Marlo, J.E., Days, E.L. *et al.* (2010) Discovery of novel allosteric modulators of metabotropic glutamate receptor subtype 5 reveals chemical and functional diversity and *in vivo* activity in rat behavioral models of anxiolytic and antipsychotic activity. *Mol. Pharmacol.*, **78**, 1105–1123.
42. Haythornthwaite, A., Stoelzle, S., Hasler, A., Kiss, A., Mosbacher, J., George, M., Bruggemann, A. and Fertig, N. (2012) Characterizing human ion channels in induced pluripotent stem cell-derived neurons. *J. Biomol. Screen.*, **17**, 1264–1272.
43. Krageloh-Mann, I., Schroth, G., Niemann, G. and Michaelis, R. (1989) The Rett syndrome: magnetic resonance imaging and clinical findings in four girls. *Brain Dev.*, **11**, 175–178.
44. Murakami, J.W., Courchesne, E., Haas, R.H., Press, G.A. and Yeung-Courchesne, R. (1992) Cerebellar and cerebral abnormalities in Rett syndrome: a quantitative MR analysis. *AJR. Am. J. Roentgenol.*, **159**, 177–183.
45. Oldfors, A., Sourander, P., Armstrong, D.L., Percy, A.K., Witt-Engerstrom, I. and Hagberg, B.A. (1990) Rett syndrome: cerebellar pathology. *Pediatr. Neurol.*, **6**, 310–314.
46. Guerrini, R. and Parrini, E. (2012) Epilepsy in Rett syndrome, and CDKL5- and FOXG1-gene-related encephalopathies. *Epilepsia*, **53**, 2067–2078.
47. Holmes, G.L. and Stafstrom, C.E. (2007) Tuberous sclerosis complex and epilepsy: recent developments and future challenges. *Epilepsia*, **48**, 617–630.
48. Goelz, M.F., Mahler, J., Harry, J., Myers, P., Clark, J., Thigpen, J.E. and Forsythe, D.B. (1998) Neuropathologic findings

associated with seizures in FVB mice. *Laboratory Animal Science*, **48**, 34–37.
49. Gogliotti, R.G., Lutz, C., Jorgensen, M., Huebsch, K., Koh, S. and Didonato, C.J. (2011) Characterization of a commonly used mouse model of SMA reveals increased seizure susceptibility and heightened fear response in FVB/N mice. *Neurobiol. Dis.*, **43**, 142–151.
50. Lindsley, C.W., Wisnoski, D.D., Leister, W.H., O'Brien, JA, Lemaire, W., Williams, D.L. Jr, Burno, M., Sur, C., Kinney, G. G., Pettibone, D.J. *et al.* (2004) Discovery of positive allosteric modulators for the metabotropic glutamate receptor subtype 5 from a series of N-(1,3-diphenyl-1H- pyrazol-5-yl)benzamides that potentiate receptor function *in vivo*. *J. Med. Chem.*, **47**, 5825–5828.
51. Kinney, G.G., O'Brien, J.A., Lemaire, W., Burno, M., Bickel, D.J., Clements, M.K., Chen, T.B., Wisnoski, D.D., Lindsley, C.W., Tiller, P.R. *et al.* (2005) A novel selective positive allosteric modulator of metabotropic glutamate receptor subtype 5 has *in vivo* activity and antipsychotic-like effects in rat behavioral models. *J. Pharmacol. Exp. Ther.*, **313**, 199–206.
52. Medrihan, L., Tantalaki, E., Aramuni, G., Sargsyan, V., Dudanova, I., Missler, M. and Zhang, W. (2008) Early defects of GABAergic synapses in the brain stem of a MeCP2 mouse model of Rett syndrome. *J. Neurophysiol.*, **99**, 112–121.
53. Gill, S.S., Pulido, O.M., Mueller, R.W. and McGuire, P.F. (1999) Immunochemical localization of the metabotropic glutamate receptors in the rat heart. *Brain Res. Bull.*, **48**, 143–146.
54. Rioult-Pedotti, M.S., Friedman, D. and Donoghue, J.P. (2000) Learning-induced LTP in neocortex. *Science*, **290**, 533–536.
55. Rioult-Pedotti, M.S., Friedman, D., Hess, G. and Donoghue, J.P. (1998) Strengthening of horizontal cortical connections following skill learning. *Nat. Neurosci.*, **1**, 230–234.
56. Sanes, J.N. (2000) Motor cortex rules for learning and memory. *Curr. Biol. CB*, **10**, R495–R497.
57. Sanes, J.N. and Donoghue, J.P. (2000) Plasticity and primary motor cortex. *Ann. Rev. Neurosci.*, **23**, 393–415.
58. Isaias, I.U., Dipaola, M., Michi, M., Marzegan, A., Volkmann, J., Rodocanachi Roidi, M.L., Frigo, C.A. and Cavallari, P. (2014) Gait initiation in children with Rett syndrome. *PloS One*, **9**, e92736.
59. Noetzel, M.J., Rook, J.M., Vinson, P.N., Cho, H.P., Days, E., Zhou, Y., Rodriguez, A.L., Lavreysen, H., Stauffer, S.R., Niswender, C. M. *et al.* (2012) Functional impact of allosteric agonist activity of selective positive allosteric modulators of metabotropic glutamate receptor subtype 5 in regulating central nervous system function. *Mol. Pharmacol.*, **81**, 120–133.
60. McLeod, F., Ganley, R., Williams, L., Selfridge, J., Bird, A. and Cobb, S.R. (2013) Reduced seizure threshold and altered network oscillatory properties in a mouse model of Rett syndrome. *Neuroscience*, **231**, 195–205.
61. Miura, K., Kumagai, T., Suzuki, Y., Ohki, T., Matsumoto, A., Miyazaki, S., Hayakawa, C., Sonta, S., Yamada, Y. and Wakamatsu, N. (2005) [Clinical symptoms of the Rett syndrome patients with MECP2 gene abnormalities]. *No to hattatsu. Brain Dev.*, **37**, 39–45.
62. Musumeci, S.A., Calabrese, G., Bonaccorso, C.M., D'Antoni, S., Brouwer, J.R., Bakker, C.E., Elia, M., Ferri, R., Nelson, D.L., Oostra, B.A. *et al.* (2007) Audiogenic seizure susceptibility is reduced in fragile X knockout mice after introduction of FMR1 transgenes. *Exp. Neurol.*, **203**, 233–240.
63. Abdala, A.P., Dutschmann, M., Bissonnette, J.M. and Paton, J.F. (2010) Correction of respiratory disorders in a mouse model of Rett syndrome. *Proc. Natl Acad. Sci. USA*, **107**, 18208–18213.
64. Castro, J., Garcia, R.I., Kwok, S., Banerjee, A., Petravicz, J., Woodson, J., Mellios, N., Tropea, D. and Sur, M. (2014) Functional recovery with recombinant human IGF1 treatment in a mouse model of Rett syndrome. *Proc. Natl Acad Sci. USA*, **111**, 9941–9946.
65. Kron, M., Howell, C.J., Adams, I.T., Ransbottom, M., Christian, D., Ogier, M. and Katz, D.M. (2012) Brain activity mapping in Mecp2 mutant mice reveals functional deficits in forebrain circuits, including key nodes in the default mode network, that are reversed with ketamine treatment. *J. Neurosci. Official J. Soc. Neurosci.*, **32**, 13860–13872.
66. Weng, S.M., McLeod, F., Bailey, M.E. and Cobb, S.R. (2011) Synaptic plasticity deficits in an experimental model of Rett syndrome: long-term potentiation saturation and its pharmacological reversal. *Neuroscience*, **180**, 314–321.
67. Hammond, A.S., Rodriguez, A.L., Townsend, S.D., Niswender, C.M., Gregory, K.J., Lindsley, C.W. and Conn, P.J. (2010) Discovery of a novel chemical class of mGlu(5) allosteric ligands with distinct modes of pharmacology. *ACS Chem. Neurosci.*, **1**, 702–716.
68. Niswender, C.M., Johnson, K.A., Luo, Q., Ayala, J.E., Kim, C., Conn, P.J. and Weaver, C.D. (2008) A novel assay of Gi/o-linked G protein-coupled receptor coupling to potassium channels provides new insights into the pharmacology of the group III metabotropic glutamate receptors. *Mol. Pharmacol.*, **73**, 1213–1224.
69. Bridges, T.M., Rook, J.M., Noetzel, M.J., Morrison, R.D., Zhou, Y., Gogliotti, R.D., Vinson, P.N., Xiang, Z., Jones, C.K., Niswender, C.M. *et al.* (2013) Biotransformation of a novel positive allosteric modulator of metabotropic glutamate receptor subtype 5 contributes to seizure-like adverse events in rats involving a receptor agonism-dependent mechanism. *Drug Metab. Disp. Biol. Fate Chem.*, **41**, 1703–1714.
70. Gregory, K.J., Herman, E.J., Ramsey, A.J., Hammond, A.S., Byun, N.E., Stauffer, S.R., Manka, J.T., Jadhav, S., Bridges, T.M., Weaver, C.D. *et al.* (2013) *N*-aryl piperazine metabotropic glutamate receptor 5 positive allosteric modulators possess efficacy in preclinical models of NMDA hypofunction and cognitive enhancement. *J. Pharmacol. Exp. Ther.*, **347**, 438–457.
71. Jones, C.K., Bubser, M., Thompson, A.D., Dickerson, J.W., Turle-Lorenzo, N., Amalric, M., Blobaum, A.L., Bridges, T.M., Morrison, R.D., Jadhav, S. *et al.* (2012) The metabotropic glutamate receptor 4-positive allosteric modulator VU0364770 produces efficacy alone and in combination with L-DOPA or an adenosine 2A antagonist in preclinical rodent models of Parkinson's disease. *J. Pharmacol. Exp. Ther.*, **340**, 404–421.